INFORMATION TO USERS

This was produced from a copy of a document sent to us for microfilming. While the most advanced technological means to photograph and reproduce this document have been used, the quality is heavily dependent upon the quality of the material submitted.

The following explanation of techniques is provided to help you understand markings or notations which may appear on this reproduction.

1. The sign or "target" for pages apparently lacking from the document photographed is "Missing Page(s)". If it was possible to obtain the missing page(s) or section, they are spliced into the film along with adjacent pages. This may have necessitated cutting through an image and duplicating adjacent pages to assure you of complete continuity.

2. When an image on the film is obliterated with a round black mark it is an indication that the film inspector noticed either blurred copy because of movement during exposure, or duplicate copy. Unless we meant to delete copyrighted materials that should not have been filmed, you will find a good image of the page in the adjacent frame.

3. When a map, drawing or chart, etc., is part of the material being photographed the photographer has followed a definite method in "sectioning" the material. It is customary to begin filming at the upper left hand corner of a large sheet and to continue from left to right in equal sections with small overlaps. If necessary, sectioning is continued again—beginning below the first row and continuing on until complete.

4. For any illustrations that cannot be reproduced satisfactorily by xerography, photographic prints can be purchased at additional cost and tipped into your xerographic copy. Requests can be made to our Dissertations Customer Services Department.

5. Some pages in any document may have indistinct print. In all cases we have filmed the best available copy.

GOODWIN, PAUL ALBERT
A THEORY FOR THE ASYMMETRY IN THE AURORAL
IONIZATION DENSITY PROFILE FOR THE GENERATION
OF AURORAL INFRASONIC WAVES.

UNIVERSITY OF ALASKA, PH.D., 1979

A THEORY FOR THE ASYMMETRY IN THE AURORAL IONIZATION

DENSITY PROFILE FOR THE GENERATION OF AURORAL

INFRASONIC WAVES

A

DISSERTATION

Presented to the Faculty of the

University of Alaska in Partial Fulfillment

of the Requirements

for the Degree of

DOCTOR OF PHILOSOPHY

By

Paul A. Goodwin, A.A., B.S., M.S.

Fairbanks, Alaska

A THEORY FOR THE ASYMMETRY IN THE AURORAL IONIZATION DENSITY

PROFILE FOR THE GENERATION OF AURORAL INFRASONIC WAVES

RECOMMENDED:

R. Parthasarathy

Charles R. Wilson

K. Jayaweera

Gary Hislason

Joseph R. Kan
Chairman, Advisory Committee

Division Head

APPROVED:

Dean of the College of Environmental Sciences

_6-3-79_
Date

K. B. Coffan
Vice Chancellor for Research and Advanced Study

April 18, 1979
Date

ABSTRACT

   Traveling pressure waves with periods from 10 to 100 seconds are
generated in the lower ionosphere by auroral electrojet current fila-
ments as they move supersonically in an equatorward direction. The
infrasonic waves produced by the auroral motions propagate to the ground
as highly directional bow waves that can be detected by infrasonic
microphones on the surface. There is an asymmetry in the reception of
auroral infrasonic waves (AIW) with respect to whether the auroral arcs
are moving equatorward or poleward.

   In the literature it is suggested that the asymmetry may be due to
anisotropic propagation conditions along the acoustic ray path from the
E-region, where AIW are produced, to the surface. Some intrinsic prop-
erty of the AIW generation mechanism itself has also been suggested as
a possible explanation. In this thesis anisotropic propagation is
eliminated as the cause of the AIW reception asymmetry.

   Theoretical calculations, beginning with a model of an auroral
precipitation region, are presented to show that there can be a signi-
ficant difference in the transverse ionization density profiles between
an auroral arc that is moving equatorward and an arc that is moving
poleward, for a given equatorward-directed E-region ambient electric
field. The calculation has been accomplished by solving the equations
of motion and continuity for the cross-sectional ionization density
profile associated with the transverse motion of a filamentary auroral
electrojet. Thus it is shown that there is an asymmetry in the ioni-
zation profiles associated with moving arcs, and in their coupling, that
is related to the relative direction of motion of the arc with respect
to the ambient electric field, and that it is this asymmetry that is
probably the cause of the observed AIW reception asymmetry.

iii

ACKNOWLEDGEMENTS

The research that led to the writing of this thesis was carried out at the Geophysical Institute under the initial guidance of Dr. Charles R. Wilson. I am deeply grateful to Dr. Wilson for not only being instrumental in the selection of the problem that I have dealt with in this thesis, but also for all the support he has given me throughout the years that I have worked with him.

At a time when I had already selected a thesis topic and had begun work on it, Dr. Joseph R. Kan was appointed my committee chairman. I thank Dr. Kan for picking up in midstream, as it were, and affording me valuable guidance in the formulation of this final version of my thesis. I feel that a substantial portion of any value that this thesis may have is a direct result of Dr. Kan's discriminating scientific judgement. I thank him for his help.

Professor R. Parthasarathy spent a great deal of time discussing with me the various aspects of the problem that I chose to deal with in this thesis. I am deeply indebted to Prof. Parthasarathy for many of the ideas that are found herein.

I would also like to thank Dr. K. O. L. F. Jayaweera and Dr. Gary Gislason, the other members of my committee, for their valuable comments and suggestions. In addition, I thank Dr. Claron Hoskins for acting as my outside examiner.

No acknowledgement section would be complete without mentioning those involved in the actual production of the thesis. I would like to extend my love, sympathy and profuse thanks to my wife Enid for putting

iv

up with all this and for typing who knows how many drafts. I would also like to thank Sandi Moseley for typing a multitude of versions of this thesis and for typing the final copy.

v

TABLE OF CONTENTS

vii

LIST OF FIGURES

viii

ix

x

CHAPTER I

AURORAL INFRASONIC WAVES: A REVIEW OF RESEARCH

1.1 INTRODUCTION

This thesis will be concerned with an extant problem in auroral infrasonic wave (AIW) research, listed by Wilson (1975), as:

1) "...the apparent asymmetry in the generation of AIW by motions of arcs parallel to $(\underset{\sim}{J} \times \underset{\sim}{B})$ but not by motions of similar arcs antiparallel to the Lorentz force direction."

Wilson (1975) also lists a second and third problem, which are presented below, but these problems will not be dealt with in this thesis.

2) "...why is the auroral source speed often much greater than the observed AIW trace velocity at the ground?"

3) "...how do the sources of high frequency auroral infrasound at 2Hz and that of AIW at 10-100 sec period differ?"

As Wilson (1975) points out, the asymmetry in the reception of AIW may be a consequence of a persistent acoustic propagation effect or it may be an intrinsic property of the generation mechanism itself. Chapter II will deal with acoustic propagation.

1

It will also be argued that winds cannot in general account for the complete north-south asymmetry observed in the reception of AIW.

Chapter III will be concerned with the AIW generation mechanism. The equations of motion of the auroral arc plasma and the continuity equation will be solved in terms of the electromagnetic field vectors, $\underset{\sim}{E}$ and $\underset{\sim}{B}$. It will be argued that the sufficient condition for the production of an AIW by an auroral event is related to: a) supersonic motion, b) the magnitude of the electric field component perpendicular to the auroral form and c) whether or not the auroral form is $E \times B$ driven.

Chapter IV will summarize. The remainder of the present chapter will be devoted to a review of AIW research.

1.2 AN INTRODUCTION TO EARLY RESEARCH

Microbarograph arrays have been situated in many locations throughout the world. These arrays have been used for various purposes and have been operational at various times. Generally set to monitor atmospheric pressure variations within a bandpass that includes infrasound, the graphic records from these microphone arrays have been used to associate the observed infrasound with theoretically feasible sources. For instance, in Boulder, Colorado, the reception of particular identifiable infrasonic waves have been correlated with the known existence of certain severe weather systems (Goerke and Woodward, 1966). In Washington, D.C., the reception of infrasound arriving from a quadrant, generally situated with a northward mean, has been correlated with

geomagnetic activity (Chrzanowski et al., 1961). In this latter case, the infrasound was thought to originate in the polar ionosphere, where geomagnetic activity is manifested in the establishment of an enlarged auroral oval and increased auroral activity.

A four-microphone quadrilateral microbarograph array has been in continuous operation, from the fall of 1965 to the spring of 1974, at College, Alaska. From 1974 to the present, the array has been operated only during the period of the year that other simultaneous geophysical data were available.

In addition to the College station (which will be denoted as COL), supplemental auroral zone infrasonic data, in support of College, have been gathered at a number of high-latitude locations at various times. In particular, supplemental station locations and operational times include: Palmer, Alaska (PAL) from October 1967 to October 1968; Inuvik, N.W.T., Canada (INV) from October 1969 to March 1971; and Stevens Village (STV) from November 1971 to April 1973.

The instrumentation used at all the auroral zone locations cited was originally developed at the National Bureau of Standards, Washington, D.C. A general description of the type of instrumentation used at these stations, as well as at stations variously located around the world, is given by Greene and Howard (1975). The COL and satellite station microbarograph arrays sample atmospheric pressure variations by utilizing an N7 electronic filter whose half-amplitude points are located in correspondence with periods of pressure variations of 9 to 70 sec, inclusively. Graphical information is recorded on time-marked

charts, with one chart for each microphone. The quadrilateral con-
figuration of the microphone array in conjunction with the time-marked
graphical display allows one to ascertain the horizontal trace velocity
and direction of travel of specific infrasonic wavefronts. Nichparenko
(1967) describes the details of the COL apparatus.

Since the fall of 1965, specific infrasonic wavepackets have been
associated with the overhead passage of certain visible auroral forms.
An example of this type of association is shown in Figure 1.1. Depicted
at the top of this figure are the COL all-sky camera photographs of a
loop surge auroral arc whose inward leading edge crossed the zenith at
0951 UT, 2 April 1973. At approximately 0959 UT, an infrasonic wave-
packet was received on the COL microbarograph array. The time shifted
and superposed graphical display of all four microphones of the COL
microbarograph array is shown at the bottom of Figure 1.1. The crite-
rion for the association of the infrasonic wavepacket and the overhead
passage of a visible auroral form is that the infrasonic wave, if it
was to have originated at the auroral arc, must be delayed by some
specified number of minutes with respect to the zenith crossing time of
the auroral form. For the event depicted in Figure 1.1, the delay time
was 8 min. A delay time close to this value would be expected if the
infrasonic wave were to have originated at ionospheric heights. Because
of the possibility of sound channeling and reflection in the various
temperature and wind regions of the atmosphere, the association crite-
rion can be expanded to include delay times in excess of 8 minutes.
However, delay times shorter than 8 minutes would suggest association
with other sources.
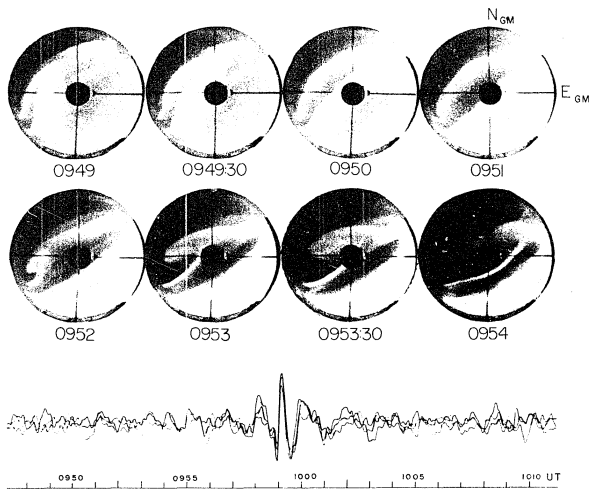
Fig. (1.1). Time shifted plot of AIW monitored by the College four microphone array on 2 April 1973. ASC photographs show the associated supersonic arc. Universal times are indicated under each ASC photograph (After Wilson, 1975).

It can be seen from Figure 1.1 that the auroral form photographed traversed the all-sky camera aperture in approximately 5 min. This corresponds to the aurora moving at 830 m/sec. The association indicated by Figure 1.1 is therefore between the supersonic motion of an auroral form and the subsequent reception of an infrasonic wavepacket. Wilson and Nichparenko (1967) showed that most infrasonic disturbances are associated with the supersonic motion of large scale auroral forms.

Analysis of available data indicates that the direction of travel of an infrasonic wavepacket closely matches the general direction of travel of the associated auroral arc. As an example, Figure 1.2 is a graphical representation of the all-sky camera photographs of Figure 1.1, as well as additional photographic data gathered at STV and Ft. Yukon (FTY). It will be noted that in Figure 1.2 the leading edge of the auroral loop surge is shown to be past the COL zenith at 0950 UT. This is consonant with the photographic evidence of Figure 1.1. Depicted in Figure 1.2 are the station locations, the location of the leading edge of the visible auroral forms, at the various indicated times, the scale, and the direction of travel of the AIW, determined at the time of its reception. The quantity denoted as ΔH is the direction of the horizontal magnetic perturbation vector for the time and station indicated. The main point of interest in Figure 1.2 is that the supersonic transversely moving auroral arcs are seen to be moving in a direction almost parallel to the direction of the indicated infrasonic packet.
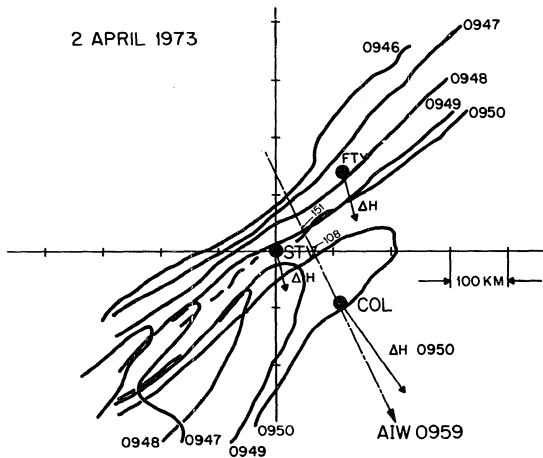
Fig. (1.2). Hand-plotted version of ASC photographs of Fig. (1.1). The stations indicated are Stevens Village, Ft. Yukon and College. The time received and direction of travel of the incoming AIW monitored at College is indicated by the dashed arrow. The vector $\triangle H$ is the total horizontal magnetic perturbation resulting from the electrojets flowing westward along the arc.

Early in 1967, Wilson and Nichparenko (1967) reported seven associations similar to that discussed above. Small numbers of such observations were reported in consequence of the difficulty in obtaining reliable simultaneous geophysical data. However, the long duration of operation of the COL microbarograph array has facilitated many more observations of the type reported by Wilson and Nichparenko. Consequently, considerable import has been added to it's usage, in the literature, of the term AIW. The use of the term is further underscored by the reception of many hundreds of infrasonic wavepackets during magnetically disturbed periods, which frequently implies the development of auroral activity. Indeed, Wilson and Nichparenko in their 1967 paper reported that over three hundred such infrasonic waves had been recorded up to the time of their writing.

Wilson (1967) suggested a shock wave model to explain the production of AIW. It was shown that a supersonic auroral form could produce acoustic waves that were amplified by superposition, provided the waves were moving in a direction corresponding to the direction of motion of the auroral form. Waves emitted in an antiparallel direction would be characterized by less superposition and, hence, considerable wavepacket spreading. In effect, Wilson's model attempted to explain the high correspondence observed between the direction of auroral arc motion and the direction of travel of the AIW. In addition, Wilson's model attempted to explain the characteristic shape of the AIW waveform and why it would not be expected to be of a continuous sinusoidal nature. The coupling mechanism, whereby the auroral form transfers

energy to the acoustic mode, was mentioned. In particular, the coupling mechanism that was dealt with by Maeda and Watanabe (1964), where the precipitating auroral electrons rapidly heated the ambient neutral atmosphere to produce an acoustic wave, was shown to be consistent with Wilson's proposed shock wave model. Consistency was also established between the shock wave model and Piddington's (1964) work on a coupling mechanism that implicated electrodynamic drift in the transfer of auroral arc kinetic energy to the acoustic mode.

1.3 LINE CURRENT INDUCTION MODELS

Wilson (1969a) developed an infinite line current induction model to examine the magnetic signatures associated with the zenith crossing of what appeared to be transversely moving filamentary electrojets. By considering the earth's surface to be an observation plane and by not including the conductivity of the earth, Wilson showed that it was possible to associate the production of AIW with the overhead passage of a moving filamentary electrojet. The association was achieved by comparing induction characteristics predicted by the model with the actual magnetic signature caused by moving filamentary current distributions. The ratio of the time developing slope of the geomagnetic vertical to horizontal component, $(Z/\Delta H)$, was compared with the same slope as predicted by the model. The model showed that line currents moving at different speeds would produce different time developing $(Z/\Delta H)$ slopes. Thus, by comparing different observed slopes with those predicted by the model, a line current velocity could be inferred. The zenith crossing

time of the filamentary electrojet could be determined since, according to the model, an extremum in the total horizontal induction would be observed at a time coincident with the zenith crossing of the line current. This time would also coincide with the time at which the Z component would be zero.

Of the eight magnetic events analysed by Wilson (1969a), using his induction model, all but one was persuasively associated with the reception of an AIW. For this one exception, the AIW was received four minutes after the zenith crossing time of the electrojet. This indicates that the generation of the specific AIW in question was associated with a portion of the electrojet that did not include the major current density that produced the magnetic record indicative of zenith crossing. The remaining seven magnetic events were clearly associated with the overhead passage of filamentary current distributions. While Wilson's (1969a) model did not result in implicit electrojet velocities that compared favorably with the associated visible auroral arc velocities, an argument was given that established that by not considering the earth's conductivity, the theoretical induction characteristics, predicted by the model, would always result in implied electrojet velocities that were too low. Based on this argument, Wilson (1969a) associated the production of AIW with the supersonic motion of certain filamentary electrojets and suggested that the supersonic motion of a current distribution was necessary for the production of infrasound.

Goodwin (1974) developed an induction model that was similar to Wilson's (1969a) but included the earth's conductivity. Comparing the time developing induction characteristics of Wilson's (1969a) model

with his own, Goodwin noted significant similarity or deviation between the two models. Goodwin found that Wilson's practice of coinciding the zenith crossing time of the filamentary electrojet with the time of an observed extremum in ΔH was in agreement with the conducting earth model. A deviation between the two models was found in the characteristic induction predicted by each. This difference was especially evident in the defined parameter, $F(t) = (Z/\Delta H)$. It was shown that, within the conducting earth model, the slope of $F(t)$, i.e., dF/dt, assumed significantly different values for each model velocity. A computer generated tabulation of dF/dt, for a range of model velocities was used in conjunction with empirical $\Delta F/\Delta t$ values, as obtained from an actual magnetic event, to result with an implied electrojet velocity. Using this method and Wilson's (1969a) original scalings, Goodwin corroborated the conclusions reached by Wilson (1969a).

1.4 AN OBSERVED ASYMMETRY IN THE RECEPTION OF AIW AND THE MORPHOLOGY
    OF THE AIW SUBSTORM

Wilson (1971) reported on an apparent asymmetry in the production
of auroral infrasound. Utilizing observations made at INV (geographic
coordinates 68° 35'N, 133°W), it was shown that the supersonic poleward
motion of certain filamentary auroral arcs did not result in the sub-
sequent reception of AIW. For two cases examined, the arcs in question
were moving at speeds, determined from all-sky camera (ASC) data, to be
1160 m/sec and 900 m/sec, respectively. At a later time, these same
arcs shifted their direction of motion to the south and subsequently
produced associable AIW. In conjunction with the zenith crossing of
these auroral arcs were the magnetic signatures indicative of fila-
mentary, westward electrojets which were moving transverse to their
long axis.

Wilson (1974) gives a listing of all observed AIW from 24 December
1965 to 30 April 1972 at COL and 16 October 1969 to 13 March 1971 at
INV. From this listing it is found that 53 out of a total of 1982 AIW
were observed at COL to have a geomagnetic northward component of veloc-
ity. That is, about 3% of observed AIW at COL were traveling northwest
or northeast with respect to the local magnetic meridian. None were
observed to be traveling due north. At INV, 6 out of a total of 272
(~2%) were observed to travel with a geomagnetic north component of
velocity. Again, none were observed to be traveling due north.

Figure 1.3 shows the number of AIW received as a function of azimuth of arrival, plotted at the locations of COL and INV with respect to the auroral oval (Fel'dshteyn, 1963) for each UT hour and each 20° of azimuthal angle (after Wilson, 1974). The length of the vectors shown in Figure 1.3 corresponds to the number of AIW received. The vectors point toward the station from the direction in which the AIW have arrived. The figure shows rather conspicuously the AIW reception asymmetry.

In the evening and midnight sectors the morphology of the AIW substorm at INV can be seen in Figure 1.3 to be about the same as that described for COL by Wilson (1969b). In the morning sector there is a pronounced difference in the number of AIW received at INV as compared with COL. Wilson (1969b; 1972) related the morning sector AIW morphology at COL to the supersonic eastward propagating "omega" bands. Wilson (1974) related the omega bands to Weins' and Rostoker's (1973) "sector" structure substorm model and showed that on the basis of that model, the number of AIW received at INV in the morning sector is expected to be lower than the number of AIW received at COL while within the same sector.

Figure 1.4 is the substorm model due to Weins and Rostoker (1973) and shows the location of the westward electrojet, with respect to the midnight meridian, associated with successive substorms. Note that in the morning sector, INV is on the average north of the electrojet while COL is south of the electrojet or directly below it. The often rapidly propagating omega bands of the midnight sector move eastward toward the
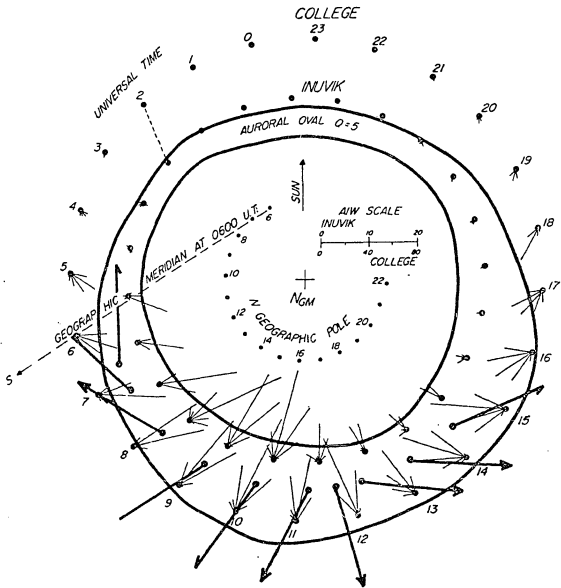
Fig. (1.3). Number of AIW as a function of azimuth of arrival ϕ, plot-
ted at the locations of College or Inuvik with respect to the auroral
oval for each hour (UT) and each 20° of ϕ. The vectors point toward
the station in the direction in which the AIW are traveling. The geo-
graphic meridian direction at each hour can be constructed by connec-
ting the station position to the location of the north geographic pole
at the same time as shown for College at 1600 UT (After Wilson, 1975).

morning sector (Akasofu et al., 1965). In so doing, they produce observable AIW at COL, which is east and south of their path but not at INV which, on the average, is east and north of their path. Evidently, supersonic auroral forms of any kind do not produce AIW if they are moving predominantly northward.

Wilson (1969b, 1971, 1974) constructed statistical tables and diagrams that showed that AIW were produced within the auroral oval and subsequently moved equatorward, past COL. The INV experiment was devised to see if a station located, at times, above or inside the northern portion of the auroral oval, could monitor poleward moving AIW. No AIW of this type were observed at INV. Wilson (1971) thus tentatively concluded that the asymmetry was intrinsic to the AIW generation mechanism and was not a consequence of the geographic location, with respect to the auroral oval, of the observer. Wilson's (1971) conclusion concerning the observed directional asymmetry in the reception of the AIW of necessity remained tentative since the research to that point in time left open two possible sources of explanation. First, there could be an asymmetric property associated with the AIW generation mechanism. Second, the asymmetry might be explained by an asymmetric property in the acoustic propagation characteristics of the polar atmosphere.
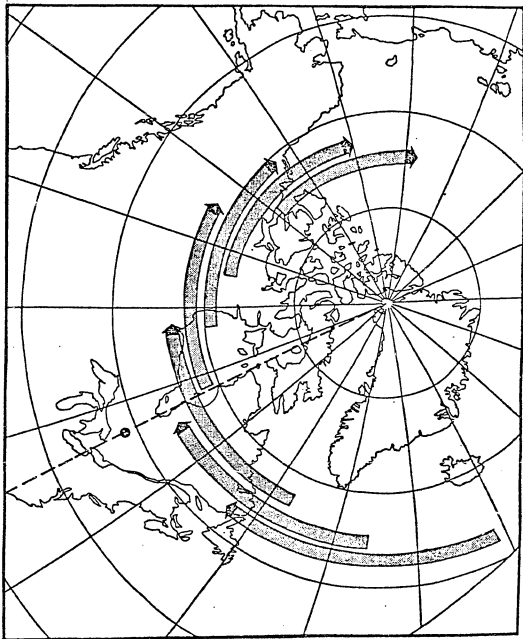
Fig. (1.4). Substorm model due to Weins and Rostoker (1973) showing the location of the westward auroral electrojet for the successive substorms with respect to the midnight meridian (dashed line) (After Wilson, 1975).

1.5 AIW GENERATION MECHANISM MODELS

Wilson (1972) incorporated the available research concerning the production of auroral infrasound into an AIW generation mechanism model that implicated electromagnetic coupling between the auroral electrojet and the ambient ionosphere as the source of the observed asymmetry in the reception of AIW. Acoustic propagation effects were excluded as a possible source of the observed asymmetry in AIW reception primarily on account of statistical evidence. As mentioned before, Chrzanowski et al., (1961) related the traveling atmospheric pressure waves they were detecting in Washington, D.C., to geomagnetic activity. The pressure waves that Chrzanowski et al., were detecting were AIW that originated some 1000 km away in the auroral zone. The fact that AIW could propagate large distances in the atmosphere then established the possibility that poleward moving AIW produced in the evening or midnight sector of the auroral oval could propagate over the polar cap to be subsequently detected in the morning sector. Wilson's (1969b, 1971, 1974) statistical data shows clearly that this does not occur (see Figure 1.3). The implication again arises that the rather common poleward moving auroral forms of the evening and midnight sectors do not produce AIW.

Examining the work of those who developed model mechanisms to explain the production of AIW, Wilson (1972) concluded that the AIW production mechanism must include electrodynamic drift as its dominant physical component. This conclusion was reached by considering the

apparent asymmetry in the production of auroral infrasound. Because of this apparent asymmetry, a Joule heat source must be excluded as the dominant AIW production component. A mechanism that stressed Joule heating should be essentially isotropic in character. Consequently, predictions arising from these model mechanisms would include the existence of poleward moving AIW, produced by poleward moving auroral arcs or electrojets. Moreover, a Joule heating mechanism of AIW production includes the possibility that a pulsating aurora can produce AIW. AIW and pulsating auroral arcs are not observed to be associated (Wilson, 1972). An example of the type of model that uses a Joule heat mechanism for AIW production is found in Maeda and Watanaba (1964) and Chimonas (1970).

Chimonas and Peltier (1970) developed a mathematical model that treated the problem of a bow wave generated by an auroral arc in supersonic motion. Both Joule heat and Lorentz force coupling was considered. The disconcerting aspect of the predictions derived from Chimonas and Peltier's model was that a relatively weak, steady current (5.4 X 10^3 amps) moving at twice the local speed of sound at a 110 km height would produce an infrasonic bow wave with an amplitude of 1 dyne/cm^2, regardless of the direction of motion. Since this prediction was also in contradiction with observation, Wilson (1972) was led to search for other processes that were subsumptive with respect to the fundamental coupling mechanisms.

Wilson (1972) proposed the ionization collection process as a secondary feature of the Lorentz force coupling mechanism. By using

this process, Wilson (1972) proposed that equatorward, supersonically traveling regions of auroral precipitation could produce corresponding regions of enhanced ion density. Northward, supersonically moving regions of auroral precipitation would produce no such corresponding region of enhanced ion concentration. Consequently, southward moving arcs will be associated with electrojets that are of sufficient ion density to, in turn, produce AIW through the coupling mechanism, provided the electrojet is moving at a supersonic speed. The poleward moving arc would not result in an AIW because ionization collection would not take place and, as a result, the ionization density would be too low.

Holt (1973) took exception to the ionization collection process proposed by Wilson (1972). He used arguments based on recombination rates and also on the consideration of the motion of plasma through the region of production unless the electric field were strictly limited to the production region. Holt concludes from his study that ionization collection, as proposed by Wilson (1972) cannot take place in an auroral arc.

Fedder and Banks, (1972) suggested that the absence of poleward moving AIW was due to a combination of three factors. These factors were: (1) Lorentz force and Joule heat terms add if the AIW source region motion is parallel to $\underset{\sim}{J} \times \underset{\sim}{B}$; (2) poleward motion of the auroral arc would result in higher Mach numbers because motion in that direction would be antiparallel to the neutral wind. The higher Mach numbers imply a diminished AIW amplitude; (3) the poleward moving arc was pro-

posed as being of greater width than the equatorward moving arc. This was thought to result in AIW with diminished amplitude.

Swift (1973) developed a mathematical model that depicted the auroral electrojet as being trapezoidal in cross-section and finite in length. The filtering characteristics of the microbarograph recording instrumentation were included. Swift's theoretically derived equations that described the pressure perturbations to be expected from a finite length, transversely moving trapezoidal current distribution, favorably matched the observed AIW waveforms. The correspondence between theory and observation was made closer by qualitatively considering the effects that dispersion would have were it included within the development of the model equations. Swift also showed that the AIW production mechanism formulations of Chimonas and Peltier (1970) and Fedder and Banks (1972) were special cases of his more general formulation.

Swift (1973) showed that a variety of observed AIW waveforms could be accounted for by considering the effects of dispersion and the instrumentation bandpass within the framework of a finite-length model electrojet. Among the observed waveforms that could be accounted for were the long wave train, the waveform with a leading negative pressure pulse, and the waveform consisting of two separate wave trains.

Concerning the apparent asymmetry in the production of AIW, Swift (1973) concluded that it may be accounted for by a combination of two circumstances. First, the Lorentz force and Joule dissipation terms, being of comparable magnitude, add when the electrojet executes equatorward motion and subtract when the electrojet is moving poleward. This

is in agreement with the earlier suggestions of Fedder and Banks (1972).
Second, Swift stated that "...the amplitude of the generated pressure
pulse decreases with increasing speed above the speed of sound. If
there exists an anti-sunward neutral wind blowing over the pole,... then
for a given velocity relative to the earth the poleward-moving electro-
jet would have a higher Mach number." However, as Swift pointed out,
the variability in the neutral wind and the possible variability in the
comparative magnitude of the Lorentz force to Joule dissipation terms
indicates that either or both of the two asymmetry arguments considered
may not be sufficient to account for the complete lack of observed
poleward moving AIW. For this reason, Swift concluded that wind shear
along the propagation path of an AIW may also have to be considered.

1.6 CURRENT PROBLEMS INVOLVED IN AIW RESEARCH

Wilson (1975) outlined the state of the current research concerning
the generation of infrasound by moving auroral forms. Apart from
considerations that have already been mentioned in this thesis, Wilson
(1975) presented a new and potentially significant observation. This
observation is manifest in the two-color photometer data of the 2
April 1973, event and in the Chatanika, Alaska, radar data for the same
event. In particular, it was shown that the primary auroral electron
spectrum is much harder in those arcs associated with the production of
AIW than it is in those arcs not so associated. For the event analyzed,
the characteristic energy of auroral electrons in the AIW associated arc

reached a maximum value of 4.0 KeV. The radar data indicated a maximum E-region electron density coincident with the maximum characteristic energy of the precipitating auroral electrons. This maximum electron density was given as 2.8×10^6 el/cm^3 at a height of 95.8 km. These values apply to universal times close to 0951 UT, 2 April 1973. Consequently, they pertain to Figures. 1.1 and 1.2 of this thesis.

In addition to an outline of the current state of research, Wilson (1975) noted the major extant problems in auroral infrasonics. These problems are listed in section 1.1. Wilson (1975) considered (1), the asymmetry problem, the most important.

The remainder of this thesis is devoted to examining the asymmetry problem in detail. The origin of the asymmetry can be considered to be manifest in either the AIW generation mechanism or in AIW propagation. In the literature, the asymmetry is currently considered as an apparent asymmetry in the AIW generation mechanism. However, the propagation problem has only been cursorily addressed. For that reason, the possible ramifications associated with AIW propagation will be examined first.

CHAPTER II

ANISOTROPIC ACOUSTIC PROPAGATION IN THE ATMOSPHERE

2.1 INTRODUCTION

The purpose of this chapter is to describe an investigation of
the possibility that the observed north-south asymmetry in the reception
of AIW is, in fact, a manifestation of an asymmetry that exists in the
acoustic propagation characteristics of the polar atmosphere.

The complete absence of observed poleward moving AIW implies that
any condition giving rise to the AIW reception asymmetry must be
exceedingly persistent. Moreover, owing to simultaneous observational
AIW experiments, conducted at a number of different latitudinal and
longitudinal locations, the extent of the condition giving rise to the
asymmetry must be, as well, large in scale. Thus, if it is assumed
that the observed asymmetry is a consequence of an acoustically aniso-
tropic atmosphere, the mechanism of the anisotropy must be temporally
stable and spacially large.

In addition to the spacial size and temporal stability of an
assumed acoustic propagation anisotropy, the mechanism of the aniso-
tropy itself must be rather pronounced. That is to say, since no AIW
are observed to move predominantly northward, significantly more
reflection, absorption or dispersion must occur along the northbound
AIW propagation path than along the corresonding southbound path.

23

The only mechanism which might result in the establishment of such a persistent, large-scale and pronounced acoustic anisotropy is wind. It is thus germane to examine the observed wind patterns of the polar atmosphere. Once the polar wind patterns are known, the acoustic anisotropy implied by those wind patterns will be assessed.

2.2 OBSERVED WIND PATTERNS IN THE POLAR ATMOSPHERE

On the 0-80 km altitude interval, ample data are available to construct accurate monthly mean wind speed and direction profiles for most areas of the earth. Since we are here interested in the propagation of AIW in the statistical sense, anomolous wind patterns of a given hour or day are of no concern. As a result, mean wind velocity profiles may be easily derived for the polar atmosphere by using one or more of the many model atmospheres that are available in the literature.

Polar wind data gathered at COL and Ft. Greely, Alaska, near COL, has been used to construct the standard atmospheres of the Handbook of Geophysics (1960) and CIRA (1965).

The variance between the model wind data of the Handbook of Geophysics and actual wind data gathered at COL is quite low on the 0-30 km altitude interval. Above 30 km the variance figures increase dramatically. However, the variance between the CIRA wind model and actual wind data, gathered at Ft. Greely, is generally low for the altitude interval from 30 km to 80 km. A low variance wind profile is thus easily constructed for the 0-80 km altitude interval, above COL, by

fitting the wind models of the <u>Handbook of Geophysics</u> and <u>CIRA</u> together at the 30 km level.

Figure 2.1 depicts the East-West (EW) windspeed profile for the representative months of January and July above COL. The wind model data of the <u>Handbook of Geophysics</u> was linearly adjusted so as to converge, at the altitude of 30 km, to the wind data of <u>CIRA</u>. The North-South (NS) component of wind has not been included in Figure 2.1 because the maximum value of this component, on the given altitude interval, is much smaller than the EW component magnitude (see also, Gregory and Manson, 1975). The ground level wind speed was arbitrarily set to zero for both profiles of Figure 2.1.

There are obvious differences between the wind patterns of January and July, the most notable of which is that the sense of the zonal flow, above the 30 km level, changes from eastward in the winter to westward in the summer. It is also seen that the zonal wind magnitude is somewhat greater during the winter than it is in the summer.

Hook (1970) reported on the observed winds at the 75-110 km level at COL. The data were based on 30.2 MHz radar observations of drifting ionized meteor trails. The data gathered by Hook (1970) pertain to observations conducted during 3 November - 20 December 1967, 2 March - 3 April 1968, and 1 June - 4 July 1968. Data were displayed for these periods as the variation in the magnitude and direction of the wind as a function of hourly local time. The striking feature of the data is that it shows a great deal of variability in the wind magnitude. The wind direction is also highly variable during the spring and summer,
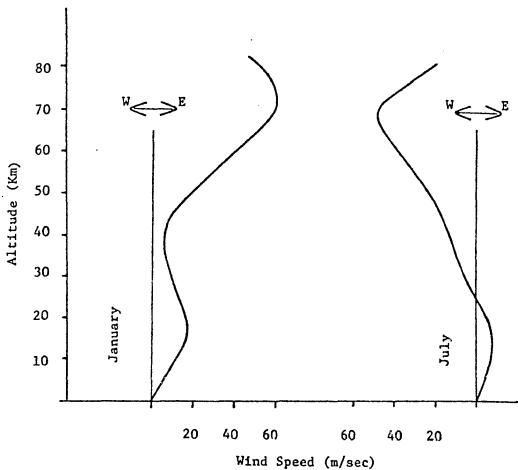
Fig. (2.1). Mean wind speed profiles for January and July above College, Alaska. Profiles are adopted from data presented in Handbook of Geophysics, 1960; CIRA, 1965, and Gregory and Manson, 1975.

but is considerably less variable during the winter. During the winter months the prevailing wind in the meteor region above COL is usually eastward and poleward. The average magnitude of the wind is approximately 40 m/sec, with a 30 m/sec standard deviation, regardless of direction. Assuming that the occurrances of wind magnitudes are normally distributed, the 30 m/sec rms variation would imply that 16% of the time, the wind would be blowing at a speed greater than 70 m/sec; about 2% of the time it would be blowing at a speed greater than 100 m/sec.

During periods of magnetic disturbance, radio wave absorption in the ionosphere occurs. Consequently, Hook's (1970) radar-derived wind data are primarily applicable to those periods not including significant magnetic activity. One would expect the neutral wind to be somewhat more aligned with respect to the current flow of the auroral electrojet if simultaneous wind data could have been gathered during magnetically active times. In fact, Hook (1970) was able to show a tendency for an enhanced equatorward neutral wind near the local midnight during magnetic disturbances.

As concerning neutral wind arising from magnetic activity, Rees (1971) reported on the drift velocities of rocket-borne chemical releases in the altitude range 90-230 km at ESRANGE Kiruna, Sweden. Photographs of a drifting trimethyl-aluminum cloud were taken from spacially separated locations. This allowed an accurate determination of the wind velocities. The chemical release experiments were conducted following both magnetically active and inactive times. Firm evidence was thus gathered to support the contention that significant ionospheric currents will cause neutral winds, often of very high magnitude within

a delay time between the onset of magnetic activity and the onset of significant winds on the order of 2-3 hours.

Reproduced in Figure 2.2 are the wind profiles provided by Rees (1971). Universal dates and times are indicated on each profile. The sense of each profile is also indicated. The coordinates are geomagnetic.

Rees (1971) gives the average horizontal magnetic perturbations at Kiruna for three hours prior to each launch. Based on this information, the wind profiles of 1 and 2 February 1968 correspond to winds that would be generated during magnetically active times. For instance, the average NS horizontal magnetic perturbation three hours prior to the 0723 UT, 4 February 1968 launch was -100γ. Two hours prior to the launch it was -100γ and one hour prior it was -50γ. The one hour average horizontal component would be indicative of E-region current intensity, much in the same way that the magnetic index Q is. The 1 November 1968 launch was conducted following a magnetically quiescent 3-hour period. However, immediately prior to the 3-hour period, intense magnetic activity was recorded. The high magnitude of the winds in the first two launches corresponds to the high magnitude of the magnetic activity three hours prior to the measurements and the relatively mild winds of the third launch correspond to low prior magnetic activity. This demonstrates the 2-3 hour delay time between the onset of substantial ionospheric currents and the establishment of significant winds in the E-region.
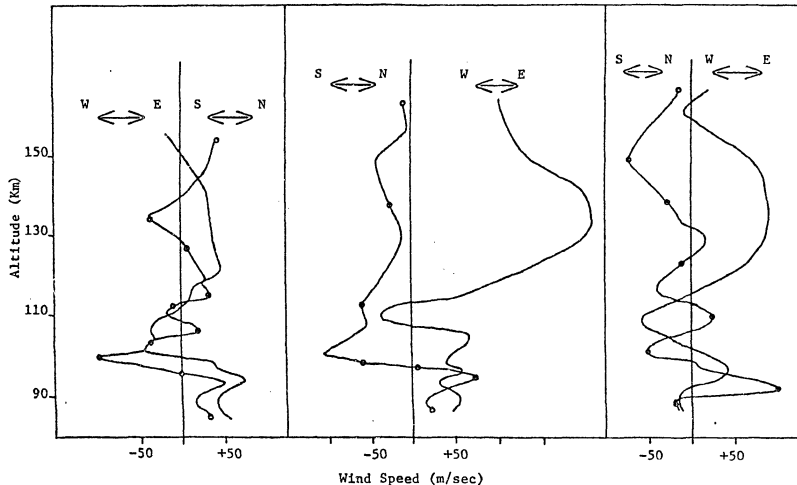
Fig. (2.2). E-region speed profiles for dates and times indicated. The profiles of 1,4 Feb 68 correspond to high magnetic activity 2-3 hrs prior to wind measurement. The profile of 1 Nov 68 corresponds to low magnetic activity 2-3 hrs prior to wind measurement (After Rees, 1971).

Neutral winds in the E-region are, evidently, quite variable. On the one hand, during low magnetic activity, a neutral wind blowing toward the northeast predominates in the ionosphere. On the other hand, 2-3 hours following the onset of intense magnetic activity, the ionospheric neutral wind blows predominantly toward the south. While the ionospheric wind is often intense, and may thus represent a source of significant acoustic anisotropy, the directional variability of the wind seems to preclude the requirement that the acoustic anisotropy, represented by the wind, be persistent.

However, AIW are coincident with the magnetically active phases of an auroral display; viz., the expansive or break-up phase and the recovery phase (see, for instance, Wilson, 1969b). Nichparenko (1967) showed that AIW are not associated with the frequently magnetically inactive quiet phase. During the expansive and recovery phases, intense westward electrojets flow (Akasofu et al., 1965; also cf. Figure 1.4). The duration of the magnetically active phases are on the order of hours. Rees' (1971) evidence concerning the 2-3 hour time delay between the onset of intense current activity and significant winds thus falls into perspective: i.e., one may assume that winds blow during AIW active periods. However, as we have seen, the velocity magnitude of the wind will probably be less than about 40 m/sec unless the substorm is well established; in which case, the wind may blow with a magnitude greater than 100 m/sec at certain altitudes.

It remains to examine the effect that these winds might have on the propagation of AIW. There is obviously an acoustic anisotropy implicit

within the wind patterns presented above, but the magnitude and stability of the anisotropy may be insufficient to account for the complete lack of observed poleward moving AIW.

2.3 THE PROPAGATION OF INFRASOUND IN THE LOWER SOUND CHANNELS OF THE POLAR ATMOSPHERE

Infrasound spectrally similar to AIW (See Appendix I) is commonly observed to propagate great distances in the polar atmosphere. For example, Harkrider (1964) and Donn and Ewing (1962) monitored, in North America, infrasound originating from the Soviet nuclear airblasts of 10 September and 30 October 1961. The epicenters of both nuclear explosions were located at Novaya Zemlya, the geographic coordinates of which are 78° 58' N, 52° 58' E. Harkrider monitored the airblast associated infrasound at, among other places, Palisades, N.Y. and Pasadena, California. Donn and Ewing monitored the infrasound at Arctic Ice Island T-3.

By comparing the theoretically calculated and observed variation of infrasonic pressure amplitude as a function of distance from the source, Harkrider (1964) was able to show that the observed infrasonic amplitude variations could be accounted for by geometrical spreading over a spherical surface. In as much as this finding was shown to be valid for over 50° of arc on the earth's surface, one could consider the infrasound as propagating along great circle ray paths, via the lower two sound channels of the atmosphere.

The great circle ray path from Novaya Zemlya (NZ) to Palisades, N.Y. passes over Greenland. The corresponding ray path from NZ to Pasadena, Ca. passes between the geographic and magnetic poles. The great circle ray path from NZ to Arctic Ice Island T-3 passes over the geographic north polar cap. The winds that must have been encountered by the infrasound as it progressed along at least one of these great circle paths did not substantially affect Harkrider's conclusion concerning the variation of infrasonic amplitude as a function of distance from the source. The winds which usually blow within the tropospheric and stratospheric sound channels apparently have little effect on the propagation of infrasound.

Also relevant to the present discussion, it has been determined that the above 10 September 1961 nuclear airblast occurred during low magnetic activity, whereas the 30 October 1961 airblast occurred during intense magnetic activity which lasted 3 hours prior to and 5 hours after the blast occurred. Thus infrasound, spectrally similar to an AIW, is observed to propagate great distances during both magnetically active and quiet times and while moving either equatorward or poleward.

Moreover, Goerke et al., (1965), have shown that volcanic infrasound can propagate great distances, in the poleward direction, through headwinds of velocity magnitude estimated to be as high as 50 m/sec. Wilson et al., (1966) and Wilson and Forbes (1969b) also dealt with volcanic infrasound. In these latter cases, infrasound propagated poleward from southcentral Alaska to COL, encountering variable winds in both sound channels which were again often as great in magnitude as 50 m/sec.

The volcanic infrasound data presented by Wilson and Forbes (1969b) shows that volcanic signals are sometimes received during AIW activity. On two occasions volcanic infrasound was recorded within about 3 hours of receiving AIW. In one case, 2 May 1968, volcanic infrasound was received beginning at 0627 UT and at 0947 UT, and an AIW was received. In the other case, 30 December 1967, volcanic infrasound was observed at 0945 UT with and AIW incoming at 1040 UT, just 55 minutes later.

Thus, it is clear that infrasound can and does propagate over large distances in the polar atmospheric sound channels while moving either poleward or equatorward and while propagating during magnetically and/or AIW active or inactive times. In view of this, Wilson's (1972) suggestion that poleward moving AIW, if produced in the evening or midnight sector, should propagate over the polar cap to be observed in the morning sector is eminently reasonable. However, as Wilson (1972) has shown, this is not observed. This indicates that if northbound AIW are in fact produced, they evidently do not enter the lower sound channels where, if they did, they would be observed.

Hence, if the AIW reception asymmetry is assumed to be a consequence of acoustic propagation, the mechanism of the asymmetry must be extant above the tropospheric and stratospheric sound channels. Among others, Press and Harkrider (1962), Diamond (1963), Pfeffer and Zarichny (1963), and Harkrider (1964) have located the upper boundary of the stratospheric sound channel in correspondence with the mesopause. Any persistent and large scale anisotropy of the polar atmosphere, of sufficient intensity to stop the propagation of northbound AIW downward,

must therefore exist at or above the mesopause, where AIW originate, if
it is to exist at all.

The high-altitude wind data presented in section 2.2 demonstrate
the possibility that an intense and large scale acoustic anisotropy may
exist in the ionosphere during many AIW active periods. In particular,
the electrojet currents implied by the magnetic activity accompanying an
AIW substorm may result in the establishment of winds or a wind shear
that preferentially reflects AIW, thus accounting for the reception
asymmetry. In the next section, we will examine the possibility of this
occurring.

2.4 THE BEHAVIOR OF ACOUSTIC WAVE NORMALS IN THE PRESENCE OF WIND

If acoustic anisotropy is held responsible for the asymmetry in the
reception of AIW, the magnitude of the anisotropy must be significant
and it must be implicit within the high-altitude wind patterns suggested
by Figure 2.2. The anisotropy may be examined by the use of a plane
wave solution, in which case the generalized eikonl equation for moving
media is applicable (Kornhauser, 1953).

As Swift (1973) has pointed out, a given portion of an AIW wave-
front is constructed from pressure contributions arising from different
segments along a finite-length electrojet source. As a result, an AIW
wavefront cannot be represented by a plane wave solution. However, if
an AIW wavefront is curvilinear, the wave will experience geometrical
attenuation, as well as absorption, as it propagates through the

atmosphere. A plane wave, on the other hand, experiences no geometrical attenuation. Thus, if the acoustic anisotropy implied by the wind patterns of Figure 2.2 are examined by using a plane wave and it is found that the anisotropy is significant, it can be said that the anisotropy will be somewhat more significant for the actual AIW. To put it another way, the direction in which a plane wave is assured of propagation will correspond to the direction in which an AIW will propagate, although the AIW will attenuate in a more pronounced fashion. The direction in which the propagation of a plane wave is impeded will correspond to the direction in which the propagation of an AIW will be more impeded. Thus, while plane wave solutions are not good approximations for actual AIW wavefronts, they are of value in assessing the acoustical anisotropy implied by the wind patterns previously presented.

In the following mathematical development, we will be primarily concerned with the effect of the E-region winds on the wave normals which are associated with the propagation of plane wave infrasound. By examining the behavior of wave normals in the presence of wind, we may infer the strength of the acoustic anisotropy implied by the wind patterns in question.

Acoustic propagation in a wind and temperature stratified atmosphere has been theoretically dealt with by Rayleigh (1945), Blokhintzev (1945), Kornhauser (1953), Landau and Lifshitz (1959) and Morse and Ingard (1968). Additional theory and empirical confirmation has been provided by Tolstoy (1957), Pidmore-Brown (1962), Press and Harkrider (1962), Donn and Ewing (1962), Pfeffer and Zarichny (1963),

Harkrider (1964) and Pierce (1965), to name but a few. Many authors
cited dealt specifically with the propagation of acoustic gravity-waves.
Consequently, most of the mathematical development which will be used
to assess the effects of E-region winds on the propagation of AIW is a
particular variation on the general subject matter already dealt with by
these authors.

Such a synthesis of available research in the field of acoustic
propagation will show that neither the E-region wind patterns in general
nor wind shear in particular can account for the complete asymmetry
observed in the reception of AIW.

The dominant filtered Fourier component of an AIW corresponds to a
wave with a 50 sec period (see Appendix I). At the sonic velocity c =
320 m/sec, this period corresponds to a plane wavelength of 16 km.
Referring to Figure 2.2, the wind in the E-region often changes sig-
nificantly within one such wavelength. To a plane wave with 16-km
wavelength, these rapidly varying wind regions would appear to be wind
shears and may thus be modeled to the first order as wind layers.

Morse and Ingard (1968: see pp. 708-714) have examined the pro-
pagation of plane waves through a wind layer. In their treatment of the
problem, mathematical expressions involving only one boundary of the
wind layer were presented. It is not difficult to extend their treat-
ment to acoustic propagaion of a plane wave entirely through the wind,
thus simulating the propagation of an AIW through the given wind regions
of Figure 2.2. Using the kinematical considerations given by Morse and

Ingard and their boundary conditions, it is found that for plane wave propagation entirely through a wind layer,

$$(2.1) \qquad \cos^{-1} (c_o/c_2) < \phi_{ip,e} \leqslant \pi/2$$

where c_o and c_2 are the sonic speeds above and below the wind layer and where $\phi_{ip,e}$ are the indicent angles of the poleward and equatorward traveling waves, respectively. A given incident angle was defined as the acute coplaner angle between the wave normal and wind velocity vector. The wind layer was considered to be a homogeneous subsonic air flow, of velocity χ, characterized by a constant sonic speed, c_1.

The condition expressed by (2.1) shows that for either the poleward or equatorward moving wave, transmission will occur independent of the wind speed, v, or thickness of the layer, provided that $v > c_1$. Any wind region in which air flow is completely horizontal may be modeled by a series of discreet wind layers. We would expect, therefore, the transmission condition expressed by (2.1) to be applicable to any wind region in which the wind speed varies only in the vertical direction. No net acoustic anisotropy is indicated by (2.1), although it is clear that a wind region can represent an obstacle for all acoustic trans-mission. That is, if $c_2 < c_o$, acoustic transmission through the wind region cannot occur.

Although not relevant to the problem concerning the AIW reception asymmetry, one can imagine wind blowing horizontally between two atmo-spheric regions of different temperature. According to the above

analysis, if the temperature above a wind region were higher than the temperature below it, an AIW originating in the higher temperature environment would not be expected to propagate through the wind to be observed at the ground. This type of situation may represent a partial explanation for the fact that not all supersonic auroral forms which move equatorward over a station zenith are associated with the subsequent reception of an AIW.

Specific wind and temperature regions which intervene between the reception and creation sites of an AIW cannot, however, account completely for the observation that the zenith crossing of some supersonic arcs are not associated with the reception of an AIW. Successive supersonic arcs have been observed to move across a station zenith such that one or more were associated with the subsequent reception of an AIW while the others were not. The large-scale characteristics of the atmosphere could not change rapidly enough to account for this type of observation on the basis of acoustic propagation alone.

In any event, the acoustic obstacle effect of a particular wind and temperature stratification, as modeled above, does not represent an acoustic anisotropy. If acoustic propagation is to be held responsible for the AIW reception asymmetry, then other mechanisms of anisotropy must be sought.

Wilson's (1975) observation that places the maximum electron density of an AIW source at the 100-km altitude level suggests, referring to the wind patterns of Figure 2.2, that AIW are possibly emitted

within, as opposed to above, a wind region. If such is the case, the situation can easily be modeled to simulate plane wave propagation.

Consider a plane wave traversing a wind region such that the wind vector and wave normal lie in the same vertical plane. Let ϕ be the acute angle between the wave normal and wind velocity vector. Let the wind blow horizontally and let the wind speed vary vertically, i.e., $v = v(z)$. As Rayleigh (1945) states:

"From Fermat's law of least time it follows that the course of a ray in a moving, but otherwise homogenous, medium is the same as it would be in a medium of which all the parts are at rest, if the velocity of propagation be increased at every point by the component of the wind-velocity in the direction of the ray."

For the situation being considered here, Rayleigh's statement postulates that the horizontal trace of the plane wave must remain constant. Mathematically,

(2.2) $\qquad c_o \sec \phi \pm v(z) = \text{constant}$

where c_o is the sonic speed of the medium. The plus and minus refer to the down and upwind propagation, respectively. The constant may be determined from initial conditions.

Consider the application of (2.2) to the case of acoustic propagation within a wind that varies in magnitude with height. In particular, consider a neutral wind that is generated by ionospheric activity. Below the generating region of this wind, one would expect the speed of air flow to taper off, provided the momentum was not maintained by some other wind generating mechanism. An approximation to this wind profile

is one that depicts the wind velocity as v = v(z) where $d^2v/dz^2 = 0$.

For such a case, dv/dz = constant. The wind profile is, hence, of the

form v(z) = az + b. If the wind magnitude is zero at $z = z_1$, and v_o at

$z = z_o > z_1$, then $a = v_o/(z_o - z_1) = v_o/\Delta z$ and $b = -v_o z_1/\Delta z$. Conse-

quently, $v(z) = (v_o/\Delta z) (z-z_1)$ = constant.

The change in the angle that the wave normal makes with the hori-

zontal may then be calculated because

$$c_o \sec \phi_o \pm v_o = c_o \sec \phi \pm (v_o/\Delta z) (z-z_1)$$

where $\phi(z_o) = \phi_o$. From this we conclude that

(2.3) $\sec \phi = \sec \phi_o \pm M (1-(z-z_1)/\Delta z)$

where $M = v_o/c_o$ (wind speed Mach number) and where the upper and lower

signs correspond to down and upwind propagation, respectively.

For wave propagation completely through the wind region, (2.3)

becomes

(2.4) $\sec \phi = \sec \phi_o \pm M$

and since $\sec \phi = \left(1-(dz/dx)^2\right)^{1/2}$

(2.5) $dz/dx = \left(1-(\sec \phi_o \pm M)^2\right)^{1/2}$

Equation (2.4) may be considered a propagation condition. Equation (2.5) is the differential equation for plane wave normals in cartesian coordinates and shows immediately that the wave normals are parallel to the horizontal whenever sec $\phi_0 \pm$ M = 1. The upper sign refers to downwind propagation. Note that neither (2.4) nor (2.5) depends on the geometry of the wind profile.

With regard to the AIW reception asymmetry, (2.5) implies that $dz/dx = 0$ occurs when the wave has propagated from its source point to the zero windspeed point and when sec $\phi_0 \pm$ M = 1. For downwind propagation, sec ϕ_0 + M = 1 and for upwind propagation, sec ϕ_0 - M = 1. However, sec $\phi_0 \geq 1$, which shows that for downwind propagation the wave normals can never be parallel to the wind.

In other words, if an acoustic wave were emitted interior to and with a wind, downward toward decreasing wind speed, such as modeled, the wind would refract the ray path to a more downward direction, thus assuring propagation through the wind region. An acoustic wave emitted within but against a wind, downward toward decreasing wind speed, would, on the other hand, tend to reflect back upward. Thus, an antisunward wind, as suggested by Swift (1973), or an equatorward wind, within which AIW are emitted, would represent an acoustical anisotropy of the type needed to explain the AIW reception asymmetry.

However, as we have seen, it would not be unusual for the iono-spheric wind to blow poleward, especially during the first few hours of a magnetic substorm. But, a poleward wind represents an acoustic anisotropy that is opposite in sense to an equatorward wind. We are

thus led to conclude that the variability of the wind direction in the
ionosphere precludes the possibility that wind can represent an acoustic
anisotropy of the type required to entirely explain the AIW reception
asymmetry.

There are other ramifications associated with the variability of
the ionospheric wind and which reflect on the asymmetry problem. For
instance, as was pointed out by Fedder and Banks (1972), if there
existed an antisunward neutral wind blowing over the pole, then for a
given velocity relative to the earth, a poleward-moving electrojet would
have a higher Mach number than an equatorward-moving electrojet. As
suggested by Fedder and Banks, and corroborated by Swift (1973), the
higher Mach number electrojets would excite a lower-amplitude pressure
wave. In as much as the amplitude of the pressure wave produced depends
on the inverse of the velocity of the electrojet with respect to the
neutrals (Swift, 1973), differences in Mach number could constitute an
explanation for the AIW reception asymmetry. However, as we have seen,
the ionospheric neutral wind often blows poleward during AIW active
periods. Hence, Fedder's and Banks' suggestion that differences in Mach
number may partially explain the AIW reception asymmetry should be
eliminated from consideration.

As previously explained, it is expected that actual AIW wave
normals will behave, in the first order sense, as do plane wave normals
while in the presence of wind. On that basis it has been shown that
while wind can account for variations in AIW trace velocity, wind
cannot, in general, account for the AIW reception asymmetry.

In view of the rather fundamental physical considerations used to derive these conclusions, there can be little doubt about their basic correctness. Nevertheless, it would be meaningful to exploit the available AIW data in an effort to validate, in whatever ways that are possible, the conclusions that have been reached.

2.5 OBSERVATIONAL EVIDENCE IN SUPPORT OF THE WAVE NORMAL ANALYSIS

In keeping with Rayleigh's (1945) postulates, as listed above, it can be inferred that acoustic refraction occurring on account of wind will tend to bend acoustic rays toward the direction in which the wind flows. Thus, while the wind regions below the mesopause (cf. Figure 2.1) are not expected to change the trace velocity of, or necessarily stop, an AIW from passing through them, they should refract an AIW such that the ray path is more aligned with the wind direction.

If this analysis is correct, the actual propagation of an AIW in the atmosphere should reflect this fact. In a prior section, it was learned that, for COL, during the month of January, the mean zonal component of wind is directed toward the east. At the 70-75 km altitude level, the magnitude of this component reaches a value of about 55 m/sec.

If AIW are produced in much the same way for each month and the above wave normal analysis is essentially correct, the prevailing winds of January should refract the ray paths of these wave-packets toward the east. This would cause the AIW to be observed coming from a more westerly direction than would be the case if no eastward wind were

blowing. Similarly, the July prevailing wind would cause a westward
refraction of the propagation path of an AIW. This would cause the AIW
to be observed coming more from the east than would be expected without
wind. Thus, the mean azimuth of arrival of AIW in January should be
west of the mean azimuth of arrival in July.

For an arbitrary three-year period beginning in 1968 and ending in
1970, the number of discrete AIW wavepackets received during January and
July were counted. Continuous infrasound was not considered because
there is too high a risk that it consists of waves constructed from
wavefronts arising from different sources. The number of these discrete
wavepackets counted, for the three years, was 63 for January and 131 for
July. The mean geomagnetic azimuth of arrival for the January signals
was found to be $-24°$, geomagnetic. That is, they arrived from the
sector west of the COL magnetic meridian. On the other hand, the mean
azimuths of arrival for the July signals was found to be $+9°$, geomag-
netic. They arrived from the sector east of the COL magnetic meridian.
These results are seen to be consonant with the expectation based on the
wind and wave normal analysis.

2.6 SUMMARY

At the outset of the present chapter, it was argued that if the AIW
reception asymmetry were a consequence of an acoustically anisotropic
atmosphere, the mechanism of the anisotropy must be temporally stable
and spacially large. Wind was said to be the only mechanism which could
meet these requirements.

The wind patterns of the polar atmosphere were thus examined. No unusual wind patterns were found to pertain to the polar tropospheric or stratospheric sound channels. However, it was found that subsequent to the onset of magnetic activity often intense wind, which was blowing roughly in the direction of the large-scale auroral electrojet, could be assumed. This represented a possible acoustic anisotropy which could become manifest during AIW active periods.

The tropospheric and stratospheric sound channels were eliminated as the seat of any intense acoustic anisotropy. The elimination was achieved by showing that infrasound, spectrally similar to AIW, is commonly observed to propagate within these sound channels, either poleward or equatorward, and during magnetically and/or AIW active or inactive times.

The possible effects of the high-altitude wind on the propagation of an acoustic wave was examined by modeling the observed wind and AIW interaction first as a constant velocity wind layer with a plane wave traveling through it. By examining the behavior of the plane wave normal at the boundary and within the wind, it was found that a constant-velocity wind layer was not representative of an acoustic anisotropy. That is, the condition for transmission through the wind layer was the same for a wave traveling downward and with the wind as it was for a wave traveling downward and against the wind. This conclusion was extended to include wave propagation through any homogeneous wind region.

The effect of a nonconstant linearly varying wind speed profile was then examined. Because of the possibility that an AIW might originate within a wind, the behavior of an acoustic wave normal was examined by using a plane wave which propagated from a point within the wind downward to a point beyond the wind. By using an argument originally formulated by Rayleigh (1945), it was shown that a plane wave originating in and propagating downward through a variable wind could reflect completely upward provided the wave were emitted against the wind. Thus, if an AIW were emitted poleward within a sufficiently intense equatorward wind, reflection could account for the asymmetry observed in the reception of AIW. However, owing to the empirical evidence that established an extreme variability in direction and magnitude of the ionospheric wind, reflection was ruled out as being the general explanation of the AIW reception asymmetry.

However, it was shown that a wind layer could represent an acoustic obstacle. Thus, it was argued that wind regions can account for, on some occasions, the observation that many supersonic auroral forms are not associated with the subsequent reception of AIW.

CHAPTER III

A THEORY FOR THE ASYMMETRY IN THE AURORAL IONIZATION DENSITY

PROFILE FOR THE GENERATION OF AURORAL INFRASONIC WAVES

3.1 INTRODUCTION

It was shown in Chapter II that the effects of wind cannot, in
general, account for the asymmetry observed in the reception of AIW. In
as much as the wind analysis of Chapter II included considerations of
acoustic propagation as well as the differences of Mach number that
would be expected of electrojets moving one way or the other through
wind, the asymmetry must be explainable on the basis of the character of
the electrojet itself. That is to say, since acoustic propagation and
the apparent relative motion of the electrojet have been eliminated as
the general source of the reception asymmetry, the asymmetry must be,
somehow, an intrinsic property of the AIW generation mechanism itself.

Models of AIW generation which are asymmetrical in nature have been
proposed. For instance, Wilson (1972) suggested that arcs moving north
as opposed to south during negative bay substorm conditions would be
characterized by significantly different ionization densities. Arcs
which moved southward would move in the direction of the ambient plasma
drift and would "collect" ionization whereas poleward-moving arcs would
not. Holt (1973) objected to Wilson's model and suggested that "ioni-
zation collection", which resulted in the ionization density differences
of the model, could not occur in conjunction with the motion of actual

47

arcs. Furthermore, Swift (1973) showed that the production of infra-
sound by a moving electrojet was dependent on the ionization number
density gradient and not on the number density alone, as Wilson had
supposed.

In developing his AIW generation model, Swift (1973) initially
assumed an electrojet with trapezoidal cross-section. At a later
point, the model was generalized to include electrojets of continuous
cross-section. The electric field within the electrojet was assumed as
transverse to the electrojet axis so that the current density depended
only on the one field component and on assumed values for the Hall and
Pedersen conductivities.

Swift (1973) showed that the supersonic motion of such electrojets
would produce infrasound. By considering the bandpass characteristics
of the equipment used to monitor AIW, Swift was able to roughly dupl-
icate many of the observed AIW waveforms. By considering the effects of
dispersion, other features of the AIW waveform were explained.

Concerning the AIW reception asymmetry, Swift (1973) showed that
the Lorentz and Joule terms of his model would add if the electrojet
moved parallel to the electric field but subtract if the electrojet
moved anti-parallel to the field. Since the two terms were of com-
parable magnitude, the effect might be of significant importance in
establishing the asymmetrical production of infrasound by moving elec-
trojets.

However, the acoustic waves produced by the motion of Swift's
(1973) electrojets greatly exaggerated the AIW amplitudes. As Swift
suggests, this indicates that certain of the internal features he had

assumed as applicable to electrojets, were overestimated in his model. It is not clear, therefore, whether or not the Joule and Lorentz terms are in fact of comparable magnitude or are of comparable magnitude only in his model. However, as Wilson (1972) suggests, the Lorentz term must be dominate because Joule heat sources, such as pulsating arcs, are not associated with the reception of AIW.

It is important to examine more thoroughly the profile and dynamics of the distribution of ionization associated with the motion of auroral arcs. Direct evidence concerning the AIW reception asymmetry was gathered by Wilson (1971, 1972), mainly at INV, during negative bay magnetic conditions and concerned the rapid motion of the so-called filamentary electrojet. The primary interest is in the ionization profiles and the internal ionization dynamics associated with these electrojets.

It is thought that since the observed reception asymmetry is complete insofar as the north-south direction is concerned, some predominant characteristic of the generation mechanism must be involved. It may be that the Joule and Lorentz terms are of comparable magnitude and are thus crucial to the final disposition of the AIW asymmetry problem. In view of Wilson's (1972) agrements, this equality is doubtful and it is probable that other factors are more important.

In any case, since some predominant characteristic of the generation mechanism must be involved in the production of AIW, we may, in the theoretical development to follow, concern ourselves primarily with the more dominant features of the electrojets which are implicated in the production of auroral infrasound. This will allow more flexibility

in simplifing the equations that must be dealt with. While a few of the
assumptions that will be used to simplify the equations cannot be said
to be truly representative, it is thought that this approach will
adequately establish a dynamically related asymmetry in the ionization
density profiles which are implicated in the generation of AIW.

In the mathematical expressions modeling the auroral electrojet
plasma, the subscripts c, n, i, and e will refer to the charged com-
ponent of the plasma, the neutral component, ion and electron, respect-
ively. The following definitions also are used:

ρ = mass density

$\underset{\sim}{V}$ = charged or neutral component velocity

$\underset{\sim}{j}$ = current density

$\underset{\sim}{B}$ = magnetic induction

$\underset{\sim}{E}$ = electric field

P = volume pressure

g = gravitational acceleration

ν = collision frequency

m = mass

e = elementary charge

N = ion, electron number density

q = ionization production function

L = ionization loss function = αN^2

γ = ratio of specific heats

k = Boltzman's constant

T = temperature

$\underset{\sim}{V}$ = precipitation region velocity (V = speed)

with the notation:

$\simeq$ "on the order of"

$\lesssim$ "less than or on the order of"

$\gtrsim$ "greater than or on the order of", etc.

MKS units will be used throughout.

We will use a cartesian coordinate system where x is positive in
the magnetic eastward direction and y is positive in the direction north
along the local magnetic meridian. Positive z will be taken as upward.
The coordinate system will be situated with respect to a region of
auroral precipitation. If the precipitation region (P-region) moves, a
primed coordinate system will be considered to move with it. In all
cases to follow, the motion of a P-region will be considered to take
place along y at a constant speed V.

If a three-fluid model for the auroral plasma is assumed, it can be
shown that the MHD equation of motion of the charged component of the
plasma is approximately equivalent to the equation of motion of the
ionic component, that is,

$$(3.1) \qquad \rho_i \frac{d\underline{v}_i}{dt} = \rho_i \frac{|e|}{m} \underline{E} + \rho_i \frac{|e|}{m} (\underline{v}_i \times \underline{B}) - \nabla P_i - \rho_i \nu_{in}(\underline{v}_i - \underline{v}_n)$$

While the use of (3.1) is seemingly inconsistent with the full MHD
approach to describing the motion of ionization of an auroral arc
plasma, Appendix II shows, mathematically, that this is not the case.
Physically, (3.1) merely emphasizes that the interaction between the
charged and neutral components of an auroral plasma is due primarily to

the ion-neutral friction. The charge neutrality assumption in the MHD
formulation is contained in the approximation used in (3.1).

The neutral component velocity of the auroral plasma was considered
to be much less than the charged component velocity. Further details
concerning the derivation of equation (3.1) may be found in Appendix II.

In the rest frame the continuity equation is of the form

(3.2) $\quad \frac{\partial}{\partial t} N_{i,e} (x, y \pm Vt, z) =$

$\quad\quad q(x, y \pm Vt, z) - L(x, y \pm Vt, z) - \nabla \cdot [N_{i,e}(x, y \pm Vt, z) \underset{\sim}{v}_{i,e}]$

where V is the constant speed of the P-region moving along the y axis.

The explicit temporal dependence (i.e., $\partial/\partial t$) of equations (3.1)
and (3.2) may be removed by transforming them to the moving frame (prim-
ed frame) according to the relations $\underset{\sim}{r} = \underset{\sim}{r} - \underset{\sim}{V}t$, $\underset{\sim}{v}'_i = \underset{\sim}{v}_i - \underset{\sim}{V}$ and $\underset{\sim}{v}'_n =$
$\underset{\sim}{v}_n - \underset{\sim}{V}$. This is possible because auroral arcs accompanied by a fila-
mentary electrojet are frequently observed to move from horizon to
horizon without significant change in form.

Thus, in the frame moving with the P-region, the following six
equations (3.3), (3.4), (3.5a), (3.5b), (3.5c) and (3.5d) form a
complete set for the six unknowns N, $\underset{\sim}{v}'_i$, $\underset{\sim}{E}'$ q, L and $\underset{\sim}{V}$ ($\underset{\sim}{r}'$, q_A, q_B,
and v_{in} are either known or invoked).

(3.3) $\rho_i(\underset{\sim}{v}'_i \nabla \cdot \underset{\sim}{v}'_i) = \rho_i \frac{|e|}{m_i} \underset{\sim}{E}' + \rho_i \frac{|e|}{m_i} (\underset{\sim}{v}'_i \times \underset{\sim}{B}) - \nabla P_i - \rho_i \nu_{in}(\underset{\sim}{v}'_i - \underset{\sim}{v}'_n)$

$$(3.4) \qquad \nabla \cdot [N_{i,e} \; \underset{\sim}{v}'_{i,e}] = q - L$$

$$(3.5a) \qquad \underset{\sim}{E}' = \underset{\sim}{E} + \underset{\sim}{V} \times \underset{\sim}{B}$$

If the P-region is considered to have width W we will use

$$(3.5b) \qquad \begin{array}{ll} q_B & (-\infty \le y' < 0) \\ q_A & (0 \le y' \le W) \\ q_B & (W < y' \le \infty) \end{array}$$

We will also use

$$(3.5c) \qquad \nabla P_i = \gamma k T \frac{\partial N}{\partial y'}$$

$$(3.5d) \qquad L = \alpha N^2$$

The collision frequencies that will be used are from Nicolet (1953) and Dalgarno (1961) and are

$$(3.5e) \qquad \nu_{in} = 4.2 \times 10^{-16} \; N_n$$

$$\nu_{ei} = [34 + 1.82 \ln (T^3/N_e)] \; N_e T^{-3/2} \times 10^{-6}$$

$$\nu_{en} = 1.5 \times 10^{-17} \; N_n T$$

In the theoretical development to follow, we will examine the charged component of the auroral plasma in the frame moving with the P-region. Consequently, equations (3.3) and (3.4) will henceforth be used. The constitutive relations, equations (3.5), will be discussed further in the context of the theoretical development.

Before solving equations (3.3) and (3.4) for the ion velocity and ion number density, it is necessary to examine the nature of a discrete auroral P-region, the characteristics of the associated electrojet, and the conditions under which they move. Of interest first is the filamentary westward electrojet and its relation to the P-region.

3.2   THE FILAMENTARY ELECTROJET

The visible arc is caused primarily by the impaction of precipitating energetic particles with the neutral constituents of the atmosphere. Apart from the excited species produced by the precipitation, ion-electron pairs are also produced. A visible auroral arc which is not in motion may therefore be considered alternatively as a region of enchanced ion-electron production.

The lifetime of, for instance, the 5577 Å neutral oxygen line is about 0.75 sec. If the P-region is moving at the speed of, say, 1000 m/sec, the 5577 Å emission region will lag behind the P-region about 0.75 km. We see that for rapidly moving arcs, the region of maximum precipitation does not exactly correspond to the region of maximum light emission, although the two regions are closely associated. Hence, for a

precipitation flux that is sufficiently intense to create visible features, the terms P-region and arc may be used synonymously. The relationship between a P-region and the filamentary westward electrojet follows.

An ionizing precipitation flux which is dumping particles onto an E-region in the presence of a westward-directed electric field can develop an associated westward electrojet. If the electrojet is magnetically observed to be filamentary, the current density will be closely associated with the P-region. To show this, one may calculate the lifetime of the ionization produced within the P-region.

As an example, consider ions and electrons to be lost by the process of recombination and consider the ion and electron number densities to be equal both inside and outside the P-region. The ionization number density can be taken to be $2.38 \times 10^{12}/m^3$ inside (Wilson, 1975) and $5 \times 10^{11}/m^3$ outside (Bryant et al., 1970). The lifetime of the enhanced ionization may be considered the time necessary for recombination to result in the transition from $N = 2.38 \times 10^{12}/m^3$ to $5 \times 10^{11}/m^3$. Since $L = \alpha N_e N_i \approx \alpha \ N^2$, and $\alpha = 3 \times 10^{-13} m^3/sec$ (Bryant et al., 1970), the ion lifetime against recombination is computed by:

$$-dN/dt = \alpha \ N^2$$

$$-(1/\alpha) \int_{N_1}^{N_2} dN/N^2 = \int_{t_1}^{t_z} dt = \tau$$

$$\tau = 5.3 \ sec.$$

It is seen that the region of enhanced ionization decays rapidly to background. This region of enhanced ionization will be expected to lag somewhat behind a moving production region unless the plasma itself has a component of velocity in the direction of the P-region motion. If the P-region is moving at the transverse speed of, say, 640 m/sec, (Mach 2 if the temperature is 250° K), the region of enhanced ionization will be about 3.4 km wider than the P-region itself.

That an electrojet associated with a transversely moving auroral arc can be considered as filamentary in nature is justified if the P-region is sufficiently narrow and if the difference between the ionization number densities inside and outside the P-region is not too great. Concerning this latter point, if the transition from $N = 10^{12}/m^3$ inside the arc to $N = 10^{10}/m^3$ outside is demanded, the lifetime of the enhanced ionization will be approximately 330 sec. Again assuming that the P-region moves at 640 m/sec, the 330 sec lifetime of the ionization could result in an enhanced ionization wake some 210 km long. However, if the P-region is narrow and the measurements of Bryant et al. (1970), for the ambient ionization number density at ionospheric heights during an auroral display (i.e., $N = 5 \times 10^{11}/m^3$) is generally valid, it is easy to visualize the possible development of a filamentary westward electrojet, the maximum current density of which will be limited to the P-region.

Accordingly, the electrojet may be considered as occupying the same area as the P-region, although, an ionization wake may develop when the P-region moves which will cause the electrojet to be somewhat off center

of the precipitation flux. For the case of a moving P-region, the arc will also lag behind but will closely duplicate the actual P-region and electrojet motion.

The primary feature of the filamentary electrojet that is of interest here is its length. Many of the arcs implicated as acoustic sources in Wilson's (1971, 1972) AIW asymmetry analysis extended from horizon to horizon on the all-sky camera photographs. The magnetogram indicated that the zenith crossing of some of these arcs were accompanied by a filamentary electrojet. This suggests that the electrojet was similarly long. Orienting the x-axis along the electrojet, this observation justifies the use of symmetry, i.e., $\partial / \partial x = 0$.

3.3 THE MOTION OF AURORAL PRECIPITATION REGIONS AND THE ASSOCIATED ELECTRIC FIELDS

The motion of a P-region has been thought to occur because: i) the precipitating particle region itself moves under the influence of E x B drift or; ii) precipitating particles dump along successive magnetic field lines. Plasma flows along the magnetic field lines in both (i) and (ii). In (i) there is a bulk motion of precipitation plasma transverse to the precipitation flux; in (ii) there is not. Therefore, (i) is indicative of objective plasma motion in the horizontally transverse direction, whereas with (ii), the horizontal transverse motion of plasma is apparent.

In principle, either a type (i) or (ii) P-region can develop an associated westward electrojet. However, there are important differ-

ences characteristic of the motion of the two types of electrojets. A type (i) electrojet objectively moves in the transverse direction. The type (ii) electrojet moves in an apparent fashion. In this latter case, the leading edge of the electrojet is created by the precipitation flux whereas the trailing edge is defined by the rapid decay of enhanced ionization. The ionized components of a type (i) electrojet move in the direction of the transverse motion of the arc. The ionized components of a type (ii) electrojet do not necessarily move in the direciton of arc motion; they may move in opposite directions.

According to Kelly et al. (1971), the poleward motions of an auroral arc during the expansive phase of a negative bay substorm cannot be the result of (i) because the observed direction of the electric field at such times and the direction of motion of the auroral arc do not correlate. The poleward moving arcs and associated filamentary westward electrojets observed during the expansive phase of a substorm by Wilson (1971, 1972) to be unassociated with AIW were, evidently, type (ii) events. On the other hand, the observations of Kelly et al. (1971), suggest that Wilson's (1971, 1972) equatorward moving arcs were of the E x B driven type (i) catagory.

Evidence has been presented by Kelly et al. (1971) for occasional decoupling of the ionospheric and magnetospheric electric fields. Thus, while the large scale electric fields suggest one E x B velocity, for equatorward moving arcs, the observed local velocity of an arc moving southward may be different. The data presented by Kelly et al. shows that the observed arc velocity is usually lower than the velocity which would be indicated by the coupled ionospheric and magnetospheric elec-

tric fields. For most auroral events, decoupled fields are, evidently, not the case, and arc motion in a given direction southward may be used to infer the magnitude of the electric field parallel to the electrojet boundary by using the E x B velocity (Bostrom, 1964). The velocity of the arc motion and hence, electrojet bulk motion, should not, however, be confused with the velocity of the constituents that make up the electrojet plasma.

In a type (i) P-region the precipitation flux may be regarded as impinging onto the ionosphere through a tube whose boundaries are defined by adjacent magnetic field lines. Within the flux tube the plasma density would be higher than without; the magnetic field line being the boundary between the two regions of differing plasma density. Clemmow et al. (1955) and Kato (1963, 1964), have shown that such a boundary will propagate with a velocity that generally differs from the velocity of the charged particles that define the boundary. Kato (1963, 1964) has pointed out that this effect arises in consequence of the polarization field which is due to the irregularities of ionization that define the boundary. Kato has shown that the polarization field superposes with the applied electric field within the boundary. This results in an electric field inside that is generally different from that outside and at the boundary. Bostrom (1964) has shown that above the 100-km altitude level, boundary velocities are suitably approximated by the E x B relation. For the situation being dealt with here, the boundary velocity is known. The E x B velocity, therefore, gives the boundary electric field but provides no conclusive information about the electric field inside the P-region or about the consequent charged component

velocities inside. Electric fields interior to a type (i) P-region and electrojet will need to be derived from observation and theory.

The electric fields associated with the apparent northward motion of a type (ii) P-region can be inferred from the measurements of Kelly et al. (1971) which typify ionospheric electric field conditions during a negative bay magnetic substorm.

Interior to each type P-region the total ionization density should be high when compared to the ambient ionization density. This would tend to raise the conductivity inside, current would be enhanced, and the ambient electric field in the direction of the current would tend to become shorted out. Therefore, the component of the electric field pointing along the electrojet should be lower inside the P-region than the corresponding component outside. This consideration also pertains to the strong filamentary electrojets examined by Wilson (1969, 1971, 1972) and Goodwin (1974), which were of a 10^4-10^5 amp magnitude.

Bostrom (1964) has shown that interior to a moving type (i) P-region (Bostrom's case 2), which is characterized by an electrojet current of I = 3 x 10^4 amps, the electric field component along the electrojet axis must be less than one-tenth the magnitude of the perpendicular component. That is, the electrojet must be predominantly a Hall current. This derived conclusion has been corroborated by the barium cloud experiments of Wescott et al. (1969).

Wescott et al.(1969) have also observationally determined that northbound arcs are associated with predominantly Hall current electrojets. Bostrom (1964) had previously shown that for a type (ii) (Bostrom's case 1) electrojet current of I = 3 x 10^4 amps to move trans-

versely along the magnetic meridian, the appropriate relation that must

exist between the wind, electric and magnetic field, which drive the

current, is: $|E_{oy} + v_{nx}B| < |E_{ox} - v_{ny}B|$ where E_{oy} is the ambient or

applied electric field perpendicular to the electrojet; E_{ox} is the

applied electric field parallel to the electrojet; v_{ny} is the perpend-

icular component of wind; v_{nx} is the parallel component of wind, and B

is the local magnetic field intensity. On the basis of the observations

of Wescott et al. (1969), the conditions derived by Bostrom (1964) to

apply to the electric fields interior to a type (i) electrojet may also

be applied to the interior electric fields of the type (ii) electrojet.

That is, the field component along the electrojet must be less than one-

tenth the field component perpendicular to the electrojet.

The detailed configuration of the electric fields that must ac-

company the motion of an electrojet through the E-region notwithstand-

ing, the validity of assuming the general applicability of the limited

observations, which concern the type of electrojet and the direction of

motion thereof, is still open to question. In other words, is it valid

to say that all poleward expansions are type (ii) in character while all

equatorward expansions are E x B driven type (i) phenomena?

The answer to this question is by no means clear. However, if

subsequent discussion is confined to the case of substorms which are

characterized by a negative magnetic bay in H, then there is ample

evidence giving the average electric field in the E-region as being

directed southwestward. If a poleward expansion occurred during such a

substorm and it was an E x B driven type (i) phenomenon, significant local electric fields antiparallel to the applied electric field would need to exist at the boundary of the north-moving flux tube. These antiparallel fields imply large perpendicular potentials. The electric field should, therefore, map to the magnetospheric equator, thus violating convection theories, similar to Mozer's and Manka's (1971), which state that a westward electric field is required at the magnetospheric equator if the substorm itself is to continue.

We might also consider the mechanisms that have been proposed to explain successive dumping.

On the one hand, magnetospheric source region particles may be perturbed by an electromagnetic wave originating in the deeper magnetoshere. The process is the well known "pitch angle scattering," ocurring by the action of an electromagnetic wave on an energetic charged particle. These waves would tend to travel along the magnetic field lines, but owing to reflection, they would also tend toward increasing L. The wave perturturbation could cause the source region particles to be successively injected along L-shells progressively northward (R. Parthasarathy, 1976, private communication). On the other hand, successive dumping may also occur because of the reconnection of oppositely directed field lines across the neutral sheet of the magnetospheric tail (Parthasarathy and Reid, 1967). In this process also, source particles would be injected along field lines successively northward. Neither mechanism allows for successive dumping equatorward.

On that basis, the observations of Kelly et al. (1971), which
failed to reveal eastward-directed electric fields during northward
expansions, indicate that their findings may be interpreted so as to
relate the poleward expansion to the successive dumping event and the
equatorward expansion to the E x B driven event. However, this does not
rule out the possibility that some equatorward expansions are type (ii)
successive dumping events. It does not matter if some are, since con-
vective theory would not be violated, although it is unclear what mech-
anism might be responsible for equatorward successive dumping.

Hence, in subsequent logical development, a synonymity will be
assumed between type (i) and equatorward motion and between type (ii)
and poleward motion. As we have seen, this is justified in the case of
the poleward expansions. In the case of the equatorward expansion, the
assumption is less justified. At a later point, the argument will be
expanded to include the possibility that some equatorward moving arcs
are in fact associated with successive dumping type (ii) P-regions.

To summarize, it has been shown in the previous two sections that
the magnetically inferred filamentary electrojet is an easily understood
phenomenon. The significant parameters in the development of an elec-
trojet that can be magnetically observed as filamentary are thought to
be the lifetime of ion-electron pairs against recombination, the width
of the P-region, and the difference between the ambient and interior
ionization number densities.

It was argued that there are two types of P-regions. The E x B
driven type (i) P-region was said to be typical of the southward motions

that occur during the negative bay of a magnetic substorm. The successive dumping type (ii) P-regions were related to the northward expansions that occur during the same magnetic substorm conditions.

Type (i) P-regions move in accordance with E x B drift, whereas the type (ii) P-region moves only in an apparent fashion owing to the precipitating plasma being dumped on magnetic field lines successively northward. It was argued that the electrojets associated with each type of P-region contained electric field components along the electrojet that are lower in magnitude than the corresponding component of the ambient, exterior electric field. Further, it was argued that the strong westward electrojets being considered here are essentially Hall currents.

3.4 THE MOMENTUM TRANSFER EQUATION

It can be seen from equation (3.3) that the dominant momentum transfer to the neutral component proceeds via the ion-neutral interaction. We will therefore drop the subscript notation of both equation (3.3) and (3.4), and proceed with the understanding that the mathematical development to follow tacitly pertains to the ion-neutral interaction.

We will first be interested in simplifying equation (3.3). The simplified equation may then be used to determine the ionic velocity.

In the case of the southbound type (i) P-region, precipitating primary ions move transversely with the locked-in magnetic field lines. In

the frame moving with the southbound P-region, the electric field seen by the ion is given by $\underset{\sim}{E}' = \underset{\sim}{E} + (\underset{\sim}{V} \times \underset{\sim}{B})$ (equation 3.5a).

For the case of the northbound type (ii) P-region, the precipitating ionization apparently moves northward but does not necessarily possess a component of velocity in that direction. The precipitating as well as produced plasma therefore responds to the electric field in the rest frame.

The variation of ionization with respect to height associated with an auroral precipitation region should reasonably match the variation predicted by, for instance, Bostrom (1964, see page 4985). That is, there will be a region of maximum ionization density. This region of maximum density varies slowly over at least a few kilometers. Thus, if the region of interest here were of unit length in the z-direction, centered about the point of maximum ionization density, terms involving $\partial N/\partial z$ could be effectively ignored on the basis of symmetry, provided that the precipitation flux remained constant. This will be assumed to be the case. Moreover, by situating the z-direction side as stated, and assuming that the precipitation flux is constant, $\partial \underset{\sim}{v}/\partial z$ may be ignored when compared to $\partial \underset{\sim}{v}/\partial y$. That is, if $\underset{\sim}{v}$ is the average ionic velocity, its magnitude and direction, for the reason of symmetry, should vary much more slowly when considered with respect to z than when considered with respect to y.

The ionization region, as previously mentioned, will be considered as infinite in extent along the x-direction (i.e., $\partial/\partial x = 0$). Transverse motion takes place along y. The x-direction side of the volume of interest will also be considered of unit length.

After the establishment of the magnetic substorm, the ambient E-region electric field is generally southwestward (Kelly et al., 1971). The magnetic field observed at ground level is represented as the earth's quiet time magnetic field with a superposed horizontal magnetic bay usually amounting to about -10^3 $\gamma = -10^{-6}$ w/m^2. The magnetic induction associated with the transverse passage of a moving auroral form that can be characterized as a westward filamentary electrojet is typically about $-400\gamma = -4 \times 10^{-7}$ w/m^2 (Goodwin, 1974). Since the earth's quiet time magnetic induction field is on the order of 5×10^{-5} w/m^2 at E-region heights, the transverse motion of the type of electrojet of interest here can be considered to only perturb the substorm induction field.

In equation (3.3), $\underset{\sim}{v} \cdot \nabla \underset{\sim}{v}$ may be expanded to read:

$$\rho \underset{\sim}{v} \cdot \nabla \underset{\sim}{v} = \rho (v'_y \frac{\partial v'_x}{\partial y'}) \; \hat{e}_x + \rho (v'_y \frac{\partial v'_y}{\partial y'}) \; \hat{e}_y + \rho (v'_y \frac{\partial v'_z}{\partial y'}) \; \hat{e}_z$$

since $\partial/\partial x' = 0$ and $\partial v'_x/\partial z' << \partial v'_x/\partial y'$, as has been stated.

With these geometrical considerations stated, equation (3.3) may be written in component form as:

(3.6a) $\quad \nu v'_x - (\frac{e}{m} B_z - \frac{\partial v'_x}{\partial y'}) \; v'_y + \frac{e}{m} B_y \; v'_z = \frac{e}{m} E'_x + \nu v'_{nx}$

(3.6b) $\quad \frac{e}{m} B_z \; v'_x + (\nu - \frac{\partial v'_y}{\partial y'}) \; v'_y + 0 = \frac{e}{m} E'_y - \frac{\gamma kt}{\rho} \frac{\partial N}{\partial y'} + \nu v'_{ny}$

(3.6c) $\quad - \frac{e}{m} B_y \; v'_x = \frac{\partial v'_z}{\partial y'} \frac{\partial v'}{\partial y'} + \nu v'_z = \frac{e}{m} E'_z$

where the neutral wind is considered to blow horizontally.

Equations (3.6) may be simplified further by comparing the order of magnitude of each term with the order of magnitude of the other terms in each component equation. Thus, it can be shown that many terms are negligible.

The net behavior and in particular the velocity of the ions will be under the influence of the crossed electric and magnetic fields within the region of interest. We may therefore write $|\underset{\sim}{v}'| \leq |\left(\underset{\sim}{E} \times \underset{\sim}{B}\right)/B|^2$ which is easily simplified. That is, Mende (1968) found evidence to suggest that upward directed electric fields, parallel to the precipitation flux, are no greater than 6 $\mu v/m$. Kelly et al., (1971) have shown that E_y θ 10^{-2}. The transformation $\underset{\sim}{E}' = \underset{\sim}{E} + \left(\underset{\sim}{v} \times \underset{\sim}{B}\right)$, shows that $E_y' = E_y$ and $E_z' = E_z$. Accordingly, $|E_z'| \ll |E_y'|$. Hence, $|v_x'| \leq |E_y'B_z/B^2|$; $|v_y'| \leq |E_x'B_z/B^2|$; and $|v_z'| \leq |E_x'B_y/B^2|$.

Assuming a dipolar magnetic field of the form given by Alfvén and Falthämmar (1963), we may calculate order of magnitude estimates for $\partial v_x'/\partial y'$, $\partial v_y'/\partial y'$, and $\partial v_z'/\partial y'$ by using the above relations for the components of $\underset{\sim}{v}'$. Expressed in terms of the primed frame, the components of the E-region dipole field are:

(3.7a) $$B_y = (3a/r_e^5)\ (r_e\cos\theta - y'\sin\theta + z'\cos\theta)$$
$$x(r_e\cos\theta + y'\cos\theta + z'\sin\theta)$$

(3.7b) $$B_z = (a/r_e^5)\ [r_e^2 - 3(r_e\sin\theta + y'\cos\theta + z'\sin\theta)^2]$$

where θ is the magnetic dipole latitude, r_e is the distance from the earth's center to the region of interest and a is the equivalent dipole

moment of the earth's magnetic field. These quantities may be taken as $r_e = 6.48 \times 10^6$ m, and $a = 8.1 \times 10^{15}$ weber-meter. Expressed in this fashion, B_z and B_y are seen to be slowly varying functions of y'. For any reasonable value of y', $r_e \cos \theta \gg$ y'sin θ; z'cos θ. Furthermore, we can set z' = 0, so that $B_y \simeq (3a/r_e^3)\sin \theta \cos \theta$ and $B_z \simeq (3a/r_e^3)$ $(1 - 3\sin^2 \theta)$. In a moving frame of reference θ is a function of time, but for the problem being considered here θ varies slowly and may be considered as a constant.

From the above expressions for B_y and B_z,

(3.8a) $\qquad B_y = 3.46 \times 10^{-5}$ w/m^2 at COL

$\qquad\qquad\quad = 2.82 \times 10^{-5}$ w/m^2 at INV

(3.8b) $\qquad B_z = -4.28 \times 10^{-5}$ w/m^2 at COL

$\qquad\qquad\quad = -7.93 \times 10^{-5}$ w/m^2 at INV

(3.8c) $\qquad B = 5.50 \times 10^{-5}$ w/m^2 at COL

$\qquad\qquad\quad = 8.42 \times 10^{-5}$ w/m^2 at INV

For motion of the northbound P-region over the range of tens of kilometers, it is clear that $|\partial B_y/\partial y'|$ and $|\partial B_z/\partial y'| \ll 1$. For motion of the southbound P-region $\partial B_y/\partial y' = \partial B_z/\partial y' = 0$ because the magnetic field is locked in. Therefore,

$$|\frac{\partial v_x'}{\partial y'}| \lesssim |\frac{B_z}{B^2} \frac{\partial E_y'}{\partial y'}|$$

$$|\frac{\partial v_y'}{\partial y'}| \lesssim |\frac{B_z}{B^2} \frac{\partial E_x'}{\partial y'}|$$

$$|\frac{\partial v_z'}{\partial y'}| \lesssim |\frac{B_y}{B^2} \frac{\partial E_x'}{\partial y'}|$$

Under steady state magnetic conditions, $\nabla \times \underset{\sim}{E} = 0$. In the southbound case, $\underset{\sim}{E}' = \underset{\sim}{E} + (\underset{\sim}{V} \times \underset{\sim}{B})$ so that $E_x = E'_x - VB_z$, $E_y = E'_y$ and $E_z = E'_z$. Also, $|E_z| << |E_y|$ and $\partial/\partial\ x = \partial/\partial x' = 0$. Consequently, $\partial E'_x/\partial y' = 0$ (northbound); $= V(\partial B_z/\partial y') = 0$ (southbound). Moreover, from Poission's equation, we find that $\partial E'_y/\partial y' \simeq e/\varepsilon_o (N_i - N_e)$. In the development of equation (3.1), Alfvén and Falthämmar (1963) assumed that $N_i = N_e$. Consequently, $\partial E'_y/\partial y' \simeq 0$. In view of previous discussion, $\partial E'_y/\partial y' \simeq 0$ is not generally valid inside an arc. However, assuming that the polarization within the arc is not too great, the expression may be taken as valid. Assuming the polarization is sufficiently low, $\partial v'_x/\partial y' \simeq \partial v'/\partial y' \simeq \partial v'_z/\partial y' \simeq 0$. In addition to simplifying equation (3.6) considerably, this result shows that for arcs moving under steady-state conditions, $dv'/dt \simeq 0$.

Continuing the simplification, consider equation (3.6b). Take the ratio of specific heats to be $\gamma = 1.4$ and $T = 250°K$. As before, let $N = 2.38 \times 10^{12}/m^3$ inside and $N = 5 \times 10^{11}/n^3$ outside, from which

$$\frac{qkT}{\rho}\ \frac{\partial N}{\partial y'}\ \theta\ \frac{\partial N}{\partial y'}\ \begin{cases} \times\ 10^{-8} & \text{(inside)} \\[2ex] \times\ 10^{-7} & \text{(outside)} \end{cases}$$

where the ionic mass was taken to be 5×10^{-26} Kg. On the other hand, $\frac{e}{m} E_y\ \theta\ 10^6 E_y$ and $\nu v'_{ny}\ \theta\ 10^5$ to 10^6. Southward directed electric fields near auroral arcs have been measured to be $\theta\ 10^{-2}$ v/m. Thus, for values of $\partial N/\partial y'$ @ 10^{10},

$$\left| \frac{\gamma kT}{\rho} \frac{\partial N}{\partial y}' \right| \ll \left| \frac{e}{m} E'_y \right|$$

and we may ignore this term on the right hand side (RHS) of equation
(3.6b). At a later point, we will further investigate the validity of
ignoring this term. This is considered important because Holt (1973)
suggests that it must be included.

Concerning equation (3.6c), it has been stated that $E'_z \leq 6$ μv/m.
Consequently, $|eE'_z/m| \lessgtr 10$. The term $| \nu v'_z | \theta |10^2 v'_z|$ and the term
$|(eB_y/m)v'_x| \theta |10^2 v'_x|$. Thus, for $|v'_x|$ or $|v'_z| > 10$, $|(eE'_z/m)/\nu v'_z|$
and $|(eE'_z/m)/eB_y/m)v'_x| \ll 1$. It is assuredly the case that $|v'_x|$ or
$|v'_z| > 10$. Hence, $|(eE'_z/m)|$ is negligible and the term may be ignored.

With the foregoing order of magnitude considerations, equations
(3.6) may be written as

(3.9a) $$\nu v'_x - \frac{e}{m} B_z v'_z + \frac{e}{m} B_y v'_z = \frac{e}{m} E'_x + \nu v'_{nx}$$

(3.9b) $$\frac{e}{m} B_z v'_x + \nu v'_y + 0 = \frac{e}{m} E'_y + \nu v'_{ny}$$

(3.9c) $$\frac{-e}{m} B_y v'_x + 0 + \nu v'_z = 0$$

Equations (3.9) are the component momentum transfer equations for the
ions of a neutral plasma. They also describe, approximately, the motion
of the charged component of a partially ionized plasma in the auroral
ionosphere.

It is implied by equations (3.9) that momentum transfer from a moving electrojet to the neutral atmosphere proceeds directly via the collision terms. Pressure does not contribute appreciably. Thus, if the ion number density profiles of the north- and south-moving filamentary electrojets of interest here are known, equations (3.9) may be used in conjunction with the collision frequency to determine the momentum transfer associated with the motion. The momentum transfer vector will be related to the wave vector of any acoustic front that might be produced by the motion of each electrojet, although superposition of wavefronts will complicate the relation. This will be discussed later. The continuity equation must first be solved so as to determine the ion number density profiles associated with the motion of a north- and south-moving electrojet.

3.5 THE CONTINUITY EQUATION

The steady-state continuity equation may be written as

$$(3.10) \qquad \nabla \cdot (N\underline{v}') = q - L$$

where q and L are the production and loss functions and are given by equations (3.5a) and (3.5b), respectively.

Expanding the left hand side (LHS) of equations (3.9), we have

$$N (\nabla \cdot \underline{v}') + \underline{v}' \cdot (\nabla N) = q - \alpha N^2$$

Because the region of interest is located at the symmetry point of N with respect to z, $|\partial N/\partial z| \ll |\partial N/\partial y'|$. Previously it was found that $\partial v_y'/\partial y' \simeq 0$. Hence,

$$(3.11) \qquad N \frac{\partial v_z'}{\partial z} + v_y' \frac{\partial N}{\partial y'} = q - \alpha N^2$$

The quantities v_y' and v_z' may be obtained from equations (3.8). They are:

$$(3.12a) \qquad v_y' = \frac{[(e/m)\ E_y' + \nu v_{ny}']\ [\nu^2 + (eB_y/m)^2] - (\nu e B_z/m)(eE_x'/m + \nu v_{nx}')}{\nu^3 + (e/m)^2\ \nu(B_y^2 + B_z^2)}$$

$$(3.12b) \qquad v_z' = \frac{(\nu e\ B_y/m)(e\ E_x'/m + \nu v_{nx}') + (e/m)^2\ B_y B_z(eE_y'/m + \nu V_{ny}')}{\nu^3 + (\frac{e}{m})^2\ \nu(B_y^2 + B_z^2)}$$

From these expressions, the function $\partial v_z'/\partial z'$, as it appears in equations (3.11), is easily obtained and is:

$$(3.13) \qquad \partial v_z'/\partial z' = 0 \quad \text{(southbound P-region)}$$
$$\simeq -(6/D)\ \nu B_y\ V \sin \theta\ (e/m)^2\ (a/r_e^5)$$
$$(r_e \sin \theta + y' \cos \theta + Z' \sin \theta) \quad \text{(northbound P-region)}$$

where D is the denominator of equations (3.12). We may therefore write equation (3.11) as

$$(3.11a) \qquad \frac{\partial N}{\partial y'} + \frac{\alpha}{v_y'}\ N^2 - \frac{q}{v_y'} = 0$$

$$(3.11b) \qquad \frac{\partial N}{\partial y'} + \frac{\alpha}{v_y'} N^2 + \frac{1}{v_y'} \frac{\partial v_z'}{\partial z} N - \frac{q}{v_y'} = 0$$

Where equations (3.11a) and (3.11b) correspond, respectively, to the southbound type (i) and northbound type (ii) P-regions.

We note that by assuming a dipolar magnetic field, the quantity $\partial v_z'/\partial z'$ was able to be calculated explicitly. However, an order of magnitude estimate of this quantity shows that the term is very small. We might then just as well have used a uniform field such that the vertical axis of the coordinate system and field direction corresponded. This would have resulted in the coefficient of N in (3.11) being zero for both the successive dumping northbound P-region and the E x B driven southbound P-region.

3.6 THE SOLUTIONS OF THE CONTINUITY EQUATION

Having determined the coefficients of the continuity equation, we are now in a position to seek solutions of the equation.

The coefficients in (3.11a, b) are not functions of N. However, they do depend on y'. If it can be shown that the coefficient of the N^2 term in equations (3.11a) and (3.11b) varies slowly with y' when compared to the coefficient of N, the equation can be identified as a standard form Riccati equation. It will thus possess analytic solutions.

How rapidly the coefficients of equations (3.11a) and (3.11b) vary with respect to y' can be inferred from the y' derivative of those quantities.

The coefficient of N^2, in equations (3.11) is $(\alpha D/n_o)$, where n_o is the numerator of (3.12a) and D is the denominator. Hence

$$\frac{\partial}{\partial y'} \; (\alpha D/n_o) = \frac{\alpha}{n_o} \; (\frac{\partial D}{\partial y'} - \frac{1}{v_y'} \frac{\partial n_o}{\partial y'})$$

where
$$\frac{\partial D}{\partial y'} = 2 \; (e/m)^2 \; v B_y \frac{\partial B_y}{\partial y'} + 2 \; (e/m)^2 \; v B_z \frac{\partial B_z}{\partial y'}$$

and
$$\frac{\partial n_o}{\partial y'} \simeq - \nu (e/m)^2 \; B_z \frac{\partial E_x'}{\partial y'} = 0$$

In the case of the southbound P-region, this expression is zero. For the case of the northbound P-region, use $E_x = -2.5 \times 10^{-2}$ v/m, $E_y = -5 \times 10^{-2}$ v/m (Kelly et al. (1971), and previously used values for the other parameters, from which it is found that $|\partial(\alpha D/n_o)/\partial y'| \; \theta \; 10^{-23}$. Clearly, the coefficient of N^2 in equation (3.11b) is an exceedingly slow varying function of y' and we may consider it as a constant.

In similar fashion, the other coefficients can be shown to vary slowly. We can therefore identify equations (3.11) as standard Riccati equations with constant coefficients and write

(3.14)
$$\frac{\partial N}{\partial y'} + PN^2 + QN - (P/\alpha) \; q = 0$$

where

(3.15)
$$P = (\alpha/v_y') = (\alpha D/n_o)$$

$$(3.16) \qquad Q = \begin{cases} 0 & \text{(southbound)} \\[2mm] \dfrac{D}{n_o} \; X & \text{(northbound)} \end{cases}$$

Writing

$$(3.17) \qquad u = \exp\left(p \int^{y'} N dy' \right),$$

equation (3.14) becomes

$$(3.18) \qquad \frac{d^2 u}{dy'^2} + Q \frac{du}{dy'} - P^2 (q/\alpha) \, u = 0$$

Total differentials have been used since, with the given approximations, $N = N(y')$.

The general solution of equations (3.18) is:

$$(3.19) \qquad u = e^{-Qy'/2} (c_1 e^{ry'} + c_2 e^{-ry'})$$

where

$$(3.20) \qquad r = \left(P^2 \frac{q}{\alpha} + \frac{Q}{4} \right)^{1/2}$$

Note that r is by definition positive.

With equations (3.17) and (3.19) it is found that

(3.21) $\qquad N = \dfrac{r}{P} \left(\dfrac{c_1\, e^{ry'} - c_2\, e^{-ry'}}{c_1\, e^{ry'} + c_2\, e^{-ry'}} \right) - \dfrac{Q}{2P}$

which is the form of a hyperbolic tangent or cotangent. Hence, if $c_1 = e^c$ and $c_2 = -e^c$, then this expression becomes a hyperbolic tangent and,

(3.22a) $\qquad N(y') = \dfrac{r}{P} \tanh(ry' + c) - \dfrac{Q}{2P}$

Similarly, if $c_1 = e^c$ and $c_2 = -e^{-c}$,

(3.22b) $\qquad N(y') = \dfrac{r}{P} \coth\,(ry' + c) - \dfrac{Q}{2P}$

By substitution, equation (3.22a) and (3.22b) are easily verified to be solutions of equation (3.14). Because of these multiple solutions, it is necessary to determine which solution corresponds to which region of interest.

3.7 SPECIALIZATION OF THE GENERAL SOLUTIONS

Solutions of the continuity and ionic momentum transfer equations have been obtained. It is the purpose of this section to specify those solutions to the cases that are descriptive of a filamentary electrojet moving through an E-region whose electromagnetic properties are typically associated with the negative bay of a magnetic substorms.

Recall that the production function q was specified as a step function. As a result, there will be three regions for which solutions must be selected. The three regions of interest correspond to $N(y' < 0)$ = $N_T(y')$; $N(0 < y' < W) = N_{IN}(y')$; $N(y' \geqslant W) = N_L(y')$. The subscripts T and L correspond to "trailing region" and "leading region", respectively.

The above designations apply to a P-region moving northward. The designations for a southward-moving P-region can be expressed in the same manner provided that the primed frame is first rotated 180° through the azimuthal angle. If this is done and the new coordinate system is denoted by double primes, it is easily inferred that

$$
\begin{aligned}
x'' &= -x' & E_x'' &= -E_x' \\
y'' &= -y' & E_y'' &= -E_y' \\
(3.23) \qquad z'' &= z' & B_y'' &= -B_y' \\
& & B_z'' &= B_z'
\end{aligned}
$$

With the given rotation, the designations N_T, N_{IN}, and N_L apply to either a north- or south-moving P-region. Note that the primed frame corresponds to the northbound type (ii) P-region while the double primed frame corresponds to the southbound type (i) P-region.

The solutions that will pertain to each region of interest will depend on the motion of ions as seen in each frame of reference. Ionic motion is given by equation (3.12) and will depend on the electromagnetic field magnitude and orientation.

Wescott et al. (1969), using barium release data, have shown that
the ambient E-region electric field during negative bay substorms
possess a component that is directed southward. The magnitude of this
component is often greater than 50 μv/m. Kelly et al. (1971) substant-
iated this observation by the use of balloon-borne electric field
measurements. Kelly *et al.* (1971) also showed that the latitudinal
component of the electric field is, on the average, directed westward
with a magnitude of about 25 μv/m. Not uncommonly it is directed
eastward but, in these cases, with a lower average magnitude.

The westward filamentary electrojets that were observed by Wilson
(1971, 1972) to be associated with AIW if they moved equatorward while
not associated with AIW if they moved poleward occurred during the
negative bay of a magnetic substorm. In view of the findings of Wescott
et al. (1969) and Kelly et al. (1971), the direction of the applied
electric field vector during Wilson's observations was, evidently,
pointing toward the southwest.

According to equation (3.12a), a southwest directed electric field
will result in a southerly flow of ions provided that

$$(3.24) \quad [\nu^2 + (eB_y/m)^2] \ (e \ E_y'/m + \nu v_{ny}') - (\nu e \ B_z/m) \ (eE_x'/m + \nu v_{nx}') < 0$$

In the primed frame, the precipitating particles are being dumped
along successive magnetic field lines. Neither the ionization produced
nor the precipitation flux necessarily moves in the direction of the
associated visible arc. In this case, the ionization responds to the

applied electric field as seen from the rest frame. Consequently, we may write equation (3.24) for the primed frame as

(3.25) $[v^2 + (eB_y/m)^2] (eE_y/m + vv'_{ny}) - (eB_z/m)(eE_x/m + vv'_{nx}) < 0$

This inequality shows that for a southwest-directed wind and electric field, ions will always drift with a southerly component of velocity when viewed in the circumstance of the primed frame. The continuity equation solution corresponding to the leading region of this frame must therefore be $N(y') = N'_B$ where N'_B is the primed frame background ionization number density. Equations (3.22) shows that $N'_B = (r/P)'_L - (Q/2P)'_L$.

The requirement that $N(y')$ not possess an absolute mimimum within the P-region, while increasing from N'_B at the leading boundary, requires that the solution involving tanh be selected as pertinent to the primed frame interior region. For the trailing region, we must select the solution involving the coth.

The primed frame solutions are then

(3.26a) $N_L(y') = N_b$

(3.26b) $N_{IN}(y') = (r/P)'_{IN} \tanh(r'_{IN}y' + c'_{IN}) - (Q/2P)'_{IN}$

(3.26c) $N_T(y') = (r/P)'_T \coth(r'_T y' + c'_T) - (Q/2P)'_T$

The constants of integration, c_{IN}' and c_T' are determined by requiring the continuity of $N(y')$ at each boundary. These boundary conditions lead to

(3.27a) $\quad c_{IN}' = \tanh^{-1} \{ (P/r)_{IN}' [N_B' + (Q/2P)_{IN}'] \} - r_{IN}' W$

and

(3.27b) $\quad c_T' = \coth^{-1} \{ (P/r)_T' [(r/P)_{IN}' \tanh(c_{IN}') + (Q/2P)_T' - (Q/2P)_{IN}'] \}$

As viewed from the circumstance of the double primed frame, the precipitating particles move in the same direction and with approximately the same speed as the associated arc and electrojet. While the area represented by the precipitation flux and the electrojet are not exactly the same, there is a substantial correspondence. For simplicity, it will be assumed that the electrojet and precipitation flux tube represent the same area, in which case the ionization of each region will respond to the same transformed electric field. Inserting $\underset{\sim}{E}' = \underset{\sim}{E} + (\underset{\sim}{V} \times \underset{\sim}{B})$ into equation (3.24) and using equation (3.23) yields

(3.28) $\quad [\nu^2 + (eB_y/m)^2] (E_y + \frac{m\nu}{e} v_{ny}') - \nu B_z [(e/m)(E_x + V B_z) + \nu v_{nx}'] > 0$

Thus, if equation (3.28) is valid, interior region ionization as seen from the double primed frame will drift southward; otherwise it will drift northward. Two distinct situations must therefore be dealt with in this frame. The case where LHS = RHS of equation (3.28) will not be

dealt with since it represents a critical situation which cannot be maintained in the motion of an actual P-region. Note that in equation (3.28) the value of E_x is related to the observed equatorward speed, V_{south}.

Case 1): If equation (3.28) is satisfied, interior region ionization will drift forward, in the direction of motion of the precipitation flux tube. Consequently, ionization produced within the P-region will not migrate outward from the trailing boundary. Rather, the produced ionization will drift forward toward the leading region. Upon migration across the forward boundary, the ionization collides with the neutrals, rapidly begins to respond to the rest frame electric fields and begins to drift with the ambient plasma. The magnitude of the drift velocity of the ambient plasma can be less than the speed of the P-region boundary (Kato, 1963; Bostrom, 1964). For those cases, plasma that migrates outward from the forward boundary is "pushed" by the advancing P-region.

We would expect, therefore, that when the conditions expressed by equation (3.28) are satisfied, the forward boundary of the advancing P-region will be characterized by a rather large ionization number density gradient. In terms of a solution for the leading region, equation (3.22b) must be selected. Equation (3.22a) will pertain to the interior region and N_T (y") = N_B'', because ionization drifts forward.

However, if leading region ionization is being swept up or pushed by the advancing electrojet, the velocity of this ionization will appear to be nearly zero if viewed from the frame moving with the P-region. If

it is assumed that the ion velocity is identically zero at this bound-
ary, then equation (3.22b) shows that the appropriate solution must be
$N_L(y'') = (q/\alpha)^{1/2} = N_B''$, which implies an infinite number density gradi-
ent at the leading boundary.

However, ions that move forward across the leading boundary, from
the interior to leading region will, for a moment, travel at the same
average speed as they did while within the interior region (the time
span is on the order of $1/\nu$). If we examine the number density profile
of the leading region just before the ions suffer massive collisions
and, hence, just before they respond to the external fields, then
(3.22b), with v_y'' specified as if it were an interior value, is appro-
priate. Selecting such a solution will more realistically represent the
leading region number density profile, although in so doing, the grad-
ients are expected to be much less than what would actually be the case
if a perfectly rectangular P-region were moving through the ionosphere
under the conditions expressed by (3.22b). The solutions of the con-
tinuity equation for this case, are, then,

(3.29a) $\qquad N_L(y'') = (r/P)_L'' \coth(r_L'' y' + c_L'')$ $\qquad (v_y'') = (v_y'')_{IN}$

(3.29b) $\qquad N_{IN}(y'') = (r/P)_{IN}'' \tanh(r_{IN}'' y'' + c_{IN}'')$

(3.29c) $\qquad N_T(y'') = N_B''$

Equations (3.22) show that N_B'' is a double-primed solution provided that $N_B'' = (r/P)_T'' + (q/\alpha)^{1/2}$. The continuity of $N(y'')$ at $y'' = 0$, W leads to

(3.30a) $c_{IN}'' = \tanh^{-1} [N_B (P/r)_{IN}'']$

(3.30b) $c_L'' = \coth^{-1}](P/r)_L'' (r/P)_{IN}'' \tanh (r_{IN}'' W + c_{IN}'')] - r_L'' W$

Equations (3.29) and (3.30) will be called solutions of the first kind.

The large number density gradients that are expected to occur in conjunction with the case where equation (3.28) is satisfied will argue strongly for the production of an AIW. This can be seen from Swift's (1973) AIW source equations which depend directly upon the number density gradient of the moving source region. However, the large gradients in the number density that are expected may also violate the previous assumption that the pressure term in the momentum transfer equation can be ignored (cf. section 3.4). When specific parameter values are adopted, corresponding number density gradients will be calculated. The probable error in ignoring the pressure term will then be discussed.

Case 2): When equation (3.28) is not satisfied, interior region ionization as seen from the south-moving double primed frame drifts northward. This means that interior region ionization will migrate outward from the trailing boundary but not from the leading boundary. In this case we expect the solutions of the continuity equation to result in number density profiles very similar to those associated with the northbound P-region. It is emphasized, however, that in the south-

bound case the plasma is moving in the general direction of the P-region motion, whereas in the northbound case, the plasma moves generally antiparallel to the P-region motion. Thus, while the number density profiles are functionally similar, the momentum transfer characteristics of the north- as opposed to the south-moving P-region will be very different.

The solutions of the continuity equation for this case are:

$$(3.31a) \qquad N_L(y'') = N_B''$$

$$(3.31b) \qquad N_{IN}(y'') = (r/P)_{IN}'' \tanh (r_{IN}'' y'' + c_{IN}'')$$

$$(3.31c) \qquad N_T (y'') = (r/P)_T'' \coth (r_T'' (r_T'' y'' + c_T''))$$

The boundary conditions lead to

$$(3.32a) \qquad c_{IN}'' = \tanh^{-1} [N_B'' (P/r)_{IN}''] - r_{IN}'' W$$

$$(3.32b) \qquad c_T'' = \coth^{-1} [(P/r)_T'' (r/P)_{IN}'' \tanh (c_{IN}'')]$$

Equations (3.31) - (3.32) will be called solutions of the second kind.

Note that the solutions of the second kind, which pertain to the southbound E x B driven P-region, are of the same form as the solutions for the northbound successive dumping P-region. Second kind solutions may therefore refer to the motion of either a type (i) or (ii) P-region, provided that equation (3.28) is invalid. Moreover, second kind solu-

tions will pertain to successive dumping P-regions moving southward, if any such P-regions exist.

The physical difference between the solutions of the first and second kind is in the direction of the net drift of ions. Drift will be controlled by the relative magnitudes of the electric and magnetic field components and by the collision frequency.

To explain, consider equation (3.28). The first term on the LHS of the inequality can be identified as the drift obtained from the ionic impetus to move in the direction of the applied electric field. The second term on the LHS can be recognized as a generalized form of the E x B drift. In solutions of the first kind, the ionic impetus to drift in the direction of the applied electric field is greater than the impetus to drift in the direction of $\underset{\sim}{E}$ x $\underset{\sim}{B}$. If the converse is true, solutions of the second kind pertain.

It is interesting to note that when either kind solutions pertain to ionic motion, electrons drift antiparallel to the applied perpendicular electric field. Thus, when solutions of the first kind are applicable, the y-direction differential velocity between ions and electrons is greater than would be expected when solutions of the second kind are applicable. Therefore, the polarization interior to the P-region should be greatest when solutions of the first kind apply to the charged component motion. Polarization would result in an additional electric field term, the effect of which is described by Kato (1963, 1964) (cf. section 3.3).

3.8 THE NUMERICAL REPRESENTATION OF THE SPECIALIZED SOLUTIONS

Most of the relevant parameters have already been specified. What will mainly be done here, then, is to provide a synopsis of the logical flow that will be used to calculate the number density profiles and momentum transfer associated with the motion of each of the two types of electrojets under consideration. Those parameter values that have not been previously defined will herein be derived or specified.

We wish to compare differences in the momentum transfer and in the variation of ion number densities that are associated with P-regions moving north as opposed to south. To facilitate the comparison, the electrojets will be defined to be similar in every respect possible, except that one moves poleward while the other moves equatorward. Therefore, the precipitation flux and, hence, the production function, q_A, must be the same for both P-regions. Moreover, the ambient production function, q_B, is required to assume the same constant value in all frames of reference.

The magnitude of q_B may be found by assuming that outside the P-region the ambient plasma remains at a constant density. The further assumption is made that the ambient plasma drift velocity remains constant within the region of interest. In that case, the continuity equation leads to $q_B = L$. Since it has already been assumed that $N_e = N_i$, $q_b = \alpha N^2$. Thus, taking the ambient ion number density to be 5×10^{11} ions/m^3 (Bryant et al. 1970), $q_B = 7.5 \times 10^{10}/\text{m}^3$ sec.

According to Wilson et al. (1975), the electron density of a particular AIW producing region is 2.38×10^{12} el/m^3. As an approximation, we may set $q_a = \alpha N_e^2$, in which case $q_a = 1.7 \times 10^{12}$/m^3 sec.

Regardless of substorm conditions, and regardless of the type of P-region under consideration, α, e, m, r_e, B_y, B_z, and θ may be taken as constants. Direct evidence concerning the asymmetry in the reception of AIW was gathered at INV (Wilson, 1971, 1972). Therefore, the quantities B_y, B_z, and θ, as listed above, will be specified at that location.

To summarize the constants, we have

$$q_A = 1.7 \times 10^{12}/m^3$$
$$q_B = 7.5 \times 10^{10}/m^3$$
$$\alpha = 3 \times 10^{-13} \ m^3/sec$$
$$e = 1.6 \times 10^{-19} \ coul$$
$$m = 5 \times 10^{-26} \ Kg$$
$$r_e = 6.48 \times 10^6 \ m$$
$$T = 250° \ K$$

Specific magnetic field values will be obtained from equation (3.8). Collision frequency is obtained from equation (3.5a) with $N_n = 2.8 \times 10^{18}$/m^3.

To determine the applied electric field components, the model requires that the southbound type (i) P-region move according to the E x B relation. Hence, $V = -E_x B_z/B^2$. The speed V is observed. The magnetic field is known. The westward component of the rest frame

electric field at the P-region boundary is therfore easily calculated. In the model, $\partial E_x' / \partial y' = 0$. Therefore, the boundary component is equivalent to the ambient westward component of the electric field.

The interior and meridional electric fields may be calculated using Bostrom's (1964) relations that relate the motion of a type (i) or (ii) P-region to the applied electric fields, the induction field and the winds. According to Bostrom (1964), currents are driven by neutral winds and/or electric fields. In his analysis, Bostrom found that if currents similar to those modeled here are to move transversely in the meridional direction, then the appropriate relations that must exist which relate the neutral wind to the electric and magnetic fields are $E_{INx} < 0.1\, E_{INy}$ (Hall current condition) and $|E_{oy} + v_{nx}B| < |E_{ox} - v_{ny}B|$ (convective condition: cf. section 3.3). The proportionality factor that will be used in connection with the Hall current condition is 0.05. The proportionality factor that will be used in connection with the convective condition is 0.9, although, arbitrarily large values of E_{oy} will be specified so as to demonstrate the asymmetry in the ionization profiles associated with arcs moving north as opposed to south.

The interior electric fields in the double primed frame are calculated as described above except they must be transformed. The relevant transformation is $E_{INx}'' = -E_x - VB_z$ and $E_{INy}'' = -E_{INy}' = -E_y'$.

Note that within the given formulation the observed speed V and the proportionality factors which were assumed in the context of Bostrom's Hall and convective conditions completely specify the electric field that must accompany the motion of either a type (i) or (ii) P-region and its associated electrojet through the ionosphere. A relation of this

sort is to be expected. Current systems cannot behave in a fashion that is completely independent of the electromagnetic properties of the medium in which they are said to move.

The ionization number density profile in the primed frame is found by inserting the above derived parameter values into the continuity equation solutions, equations (3.26) – (3.27), and the appropriate constitutive equations, equations (3.15) and (3.16) with equation (3.12).

The number density profile in the double primed frame is calculated by first testing the observed value of V within the context of equation (3.28). If the inequality is valid, solutions of the first kind, equations (3.29) – (3.30), are used to calculate the profile. If the inequality is not valid, solutions of the second kind, equations (3.31) – (3.32), must be used.

The momentum transfer of each type P-region through the same environment is calculated in accordance with equation (3.8) and the number density profiles. That is to say, momentum transfer per unit volume = $mN\nu(\underline{v}_i - \underline{v}_n)$, where the momentum being transferred by the ambient plasma to the neutral atmosphere is to be subtracted. We note that within such a formulation, the momentum transfer and number density profiles will be of the same functional form.

In addition, the model pressure-gradient term, $(\gamma kT/mN) \, \partial N/\partial y'$, which was taken to be negligible in the mathematical development, may be calculated using the appropriate number density profile derivatives. By calculating this term for each point along the number density profile, it may be compared with the criterion by which it was originally ignored.

In any event, the pressure term may be used in conjunction with the collision terms to calculate the net interaction of the P-region plasma with the neutral atmosphere.

3.9   THE IONIZATION NUMBER DENSITY AND MOMENTUM TRANSFER PROFILES
        THAT ARE ASSOCIATED WITH THE MERIDIONAL MOTION OF AURORAL
        ARCS AND A DISCUSSION CONCERNING THE DYNAMICS OF THE MOTION

Using the foregoing logical flow as a guide in programming, the relevant solutions were evaluated by the use of a computer. Although cumbersome, plasma number density and hence momentum transfer profiles were obtained in a straightforward manner. The following figures depict the results of the calculations for a number of specific situations.

Figures 3.1 and 3.2 are calculated from equations (3.26) – (3.27) and equations (3.29) – (3.30), respectively. They depict the number density and hence, momentum transfer profiles that are expected to occur in conjunction with the meridional motion of a step function precip- itation region through the ionosphere during a magnetic substorm. Figure 3.1 pertains to the successive dumping northbound P-region while Figure 3.2 pertains to the E x B driven southbound P-region. In both cases, the associated visible arc would appear on the ground to be moving at the commonly observed speed of 1000 m/sec in the direction indicated for the P-region motion.

The electric fields indicated apply to the stationary or obser- vation frame. The neutral wind was assumed to be blowing toward the
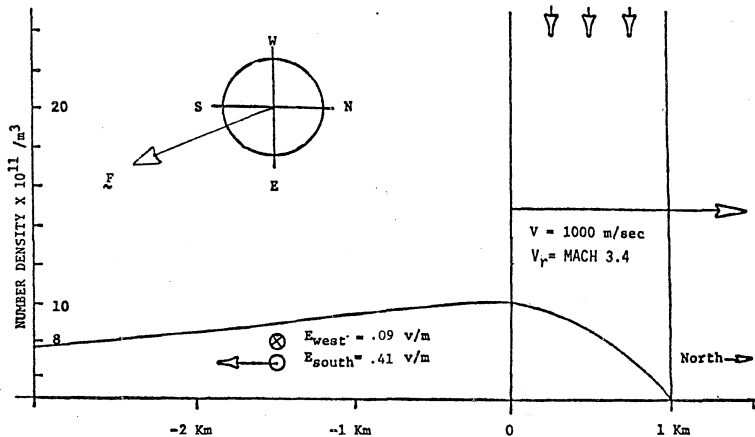
Fig. (3.1). The ionization number density profile associated with a successive dumping precipitation region moving due north at 1000m/sec. The wind is toward the south and west at 100 m/sec, respectively. The electric fields indicated pertain to the observation frame. The vector $\underset{\sim}{F}$ indicates the force exerted by a unit-face volume of the forward region plasma on the neutral atmosphere: $\underset{\sim}{F} = (2.6E-3, S23°E)$.

Fig. (3.2). The ionization number density profile associated with an E x B driven precip-
itation region moving due south at 1000 m/sec. The wind is toward the south and west at
100 m/sec , respectively. The electric fields indicated pertain to the observation frame.
The vector $\underline{F}$ indicates the force exerted by a unit-face volume of the forward region plasma
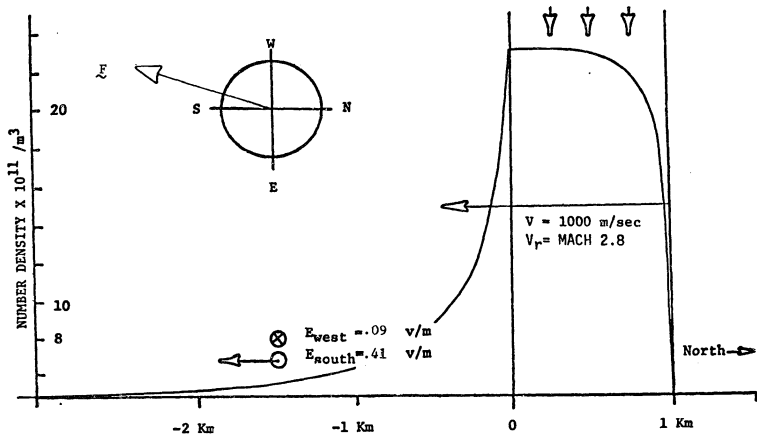on the neutral atmosphere: $\underline{F}$ = ($\gg$8.1E-3, S18°W).

south at 100 m/sec and toward the west at 100 m/sec. It will be shown
later that the inclusion of wind does not significantly alter the pro-
files. Pictured in the upper left hand corner is a geomagnetic co-
ordinate system, the north-south axis of which corresponds to the same
axis of the larger figure. The east-west axis of the larger figure is
perpendicular to the page. Indicated with the smaller coordinates is
the vector $\underline{F}$. This vector represents the total force exerted on the
neutral atmosphere by arbitrary, equal volumes, of unit-face, through
the leading region of each profile. The magnitude and direction of this
vector is given in the captions of each figure.

A number of differences are immediately apparent upon comparing the
two profiles, the most obvious of which is the difference in the maximum
number density. That is, the southbound F-region is characterized by a
maximum number density which is about a factor of 2 larger than is the
case for the northbound F-region.

Physically, when F-regions move through the stipulated environment,
both the north- and south-moving regions lose ionization owing to ion
drift velocities which are different from the velocity of the F-region
itself. The plasma drift velocity as seen from the frame moving with
the northbound successive dumping F-region is large and negative. The
higher the speed poleward, the faster the produced plasma would appear
to drift equatorward. Thus, in the northbound case, produced plasma is
being swept out of the trailing boundary and produces a rather long wake
of enhanced ionization.

This is contrasted to the case where an E x B driven electrojet
moves equatorward through the same environment. Here, produced plasma

is swept out of the advancing P-region through either the leading or trailing boundaries, depending upon whether the interior region drift velocities are positive or negative (cf. equation (3.28)). Depicted in Figure 3.2 are solutions of the first kind, indicating that the produced plasma, as seen from the frame moving with the P-region, is drifting in the direction of P-region motion. Consequently, ionization tends to be swept out of the forward boundary. However, as we have seen, the migration of plasma across this boundary is impeded by the electro-magnetic properties that must exist at the boundary, and which imply drift speeds lower than the interior region ion speed. While produced ionization can be expected to drift outward from this boundary, the flux would be significantly lower than is the flux associated with the trailing boundary of the northbound P-region.

Hence, rather than saying the southbound P-region collects ion-ization (Wilson, 1972), it should be said that the southbound P-region "retains" produced plasma more affirmatively than does the northbound P-region. Moreover, this effect will become more apparent the faster the P-regions move.

The second difference in the profiles associated with P-regions moving north as opposed to south is seen from the slope of the advancing forward edge. Swift's (1973) AIW source equations show that the pres-sure perturbations produced in conjunction with the motion of a current distribution depends primarily on the slope of the forward edge. The forward edge of the electrojet produces the positive pressure pulse usually observed in connection with the reception of an AIW. Swift

showed that the rearward region and its geometry contribute little to the form of the observed pressure perturbation.

Hence, if the particular E x B driven southbound P-region depicted in Figure 3.2 were to be associated with the production of an observable AIW, the successive dumping northbound P-region could not be, because the average slope of the advancing forward edge is, in the latter case, orders of magnitude less than is the case for the southbound P-region. The motion of the particular current distributions depicted in Figures 3.1 and 3.2 thus implies a rather easily assessed first order asymmetry in the production of an AIW.

It is emphasized that the current distributions under consideration are filamentary westward electrojets of the same intensity. They are moving through the same ambient environment and the production function of one is the same as the other. At ground level, if one were observed to have an associated visible arc, so would the other. Both electrojets would imprint a magnetogram with the signature indicative of the transverse motion of a line current. To the extent that the filamentary electrojets and the accompanying arcs observed by Wilson (1971, 1972) at INV, to be associated with AIW if they moved equatorward while not associated with AIW if they moved poleward, can be represented as being in conjunction with the motion of a 1-km wide step production function P-region, the theory developed herein and observation are in agreement.

If the P-region under consideration were wider, say 10 km instead of 1 km, the effect would be to markedly increase the maximum ionization number density within the northbound interior region and also to in-

crease the length of the ionization wake associated with the northbound case. This effect is shown in Figure 3.3 which corresponds to the same situation as depicted by Figures 3.1 and 3.2, except that the P-region is wider.

The reason that the northbound P-region is now characterized by a higher maximum number density is because plasma produced at the leading boundary takes a longer time to exit the P-region through the trailing boundary. Since the produced plasma remains within the P-region longer, the interior can become characterized by a higher number density.

The increased length of the wake occurs because a longer time is required for the increased ionization density to decay to background.

It is noted from Figure 3.3 that the slope of the forward edge is not much affected by increasing the width of the P-region. Hence, if the southbound P-region of this case were implicated in the production of an observable AIW, we would still not expect the northbound P-region to be likewise implicated.

The northbound electrojet represented in Figure 3.3 might still be magnetically observed as filamentary in character, although, if the electrojet were much wider it could not be.

If the P-regions presently under consideration were represented by a continuous production function instead of a step production fuction, the conclusion that the southbound P-region is characterized by much higher number density gradients along the forward edge than is the northbound P-region remains valid.

To see why this is the case, consider that the ionization profile of Figure 3.2 is little different from the profile that would be
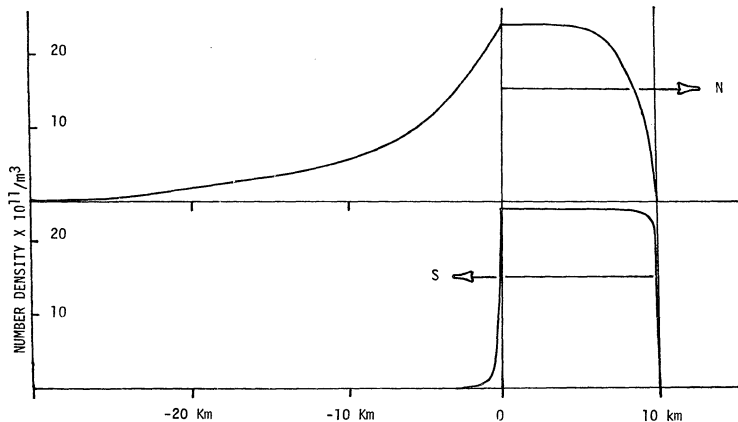
Fig. (3.3). Top and bottom profiles same as Fig's. (3.1) and (3.2), respectively, except that the width of the precipitation region is 10 Km.

expected if the P-region were not moving at all. Figure 3.4 gives an example of a stationary P-region situated within an ionosphere where the wind velocity is the same as has been previously assumed. We note the similarity between the two profiles and recall that the forward edge of the profile of Figure 3.2 indicates a slope much less than would be expected if an actual step function P-region were moving through the ionosphere such that solutions of the first kind were applicable.

In other words, to the extent that E-region conditions conform to the validity of equation (3.28), it would appear that the external deformation of the P-region production function is minimal even when the P-region moves very rapidly. Interior to the P-region, however, deformation is expected. When solutions of the first kind are appropriate, produced plasma drifts forward in the direction of motion of the P-region. Upon encountering the leading or, in this case, southward boundary, the plasma is impeded in its forward motion because of the electric field, and implicit drift velocity, that must exist at that boundary if the motion of the P-region is to be accounted for. Hence, produced plasma would tend to pile up at that boundary, resulting in higher number density gradients than would otherwise be the case.

This dynamical behavior of the southbound type (i) P-region is to be compared with the northbound type (ii) P-region. A comparison of Figures 3.1 and 3.4 suggests that if the P-region successively dumps poleward, the production function is significantly distorted, in a manner which will decrease the number density gradients of the leading boundary. Moreover, the faster the P-region moves, the more pronounced the effect becomes.

Fig. (3.4). Same as Fig's. (3.1) and (3.2) except that the precipitation region is stationary.

We conclude, therefore, that regardless of the type of production function that is characteristic of an actual P-region, if the P-region successively dumps poleward, the leading edge number density gradients will significantly decrease. If the P-region is E x B driven and ionospheric conditions are such that equation (3.28) is valid, the leading edge number densities will significantly increase. Thus, if the E x B driven type (i) P-region is implicated in the production of an observable AIW, then the corresponding successive dumping type (ii) P-region cannot be.

The differences expected in the number density gradients are physically less important than are the differences in momentum transfer between the north- and south-moving electrojets. The E x B driven electrojet of Figure 3.2 transfers forward region momentum in the direction of its transverse motion. The successive dumping electrojet of Figure 3.1 is transferring forward region momentum in a direction with components antiparallel to its transverse motion. Moreover, the momentum transfer associated with the E x B driven electrojet motion is at least an order of magnitude greater than is the case for the successive dumping electrojet.

The momentum transfer vector associated with an arbitrary section of the P-region will be related to the wave vector of any acoustic wave which is produced in front of the advancing P-region. Superposition and energy transfer into the positive pulse wave mode will cause the wave vector magnitude and direction to differ from the magnitude and direction of the momentum transfer vector associated with a given section of the P-region. Nevertheless, the direction of the two vectors will

roughly correspond. For the particular electrojets implicit in the profiles of Figures 3.1 and 3.2, if the southbound electrojet produced an acoustic wave, it would subsequently be observed at ground level to be traveling in the general direction of the associated visible arc. If the northbound electrojet produced an acoustic wave, its wave vector would possess components antiparallel to the electrojet's transverse velocity. If it were subsequently observed at ground level, this AIW could not be associated, in the usual sense, with the motion of the electrojet or its arc.

The magnitude and direction of the momentum transfer vector is crucial to the association of AIW with a given arc. It is, therefore, important to examine this vector for electrojet motion in the entire velocity range above Mach 1, where the production of an AIW is feasible. Figures 3.5 and 3.6 show the number density profiles and leading region momentum transfer of P-regions (as indicated by P_A in each figure) whose associated arcs would be observed to be moving at the transverse speed of 352 m/sec. The wind was assumed to be zero so that both P-regions are moving at Mach 1.1, with respect to the neutrals. For reference, Figures 3.7 and 3.8 depict the same P-regions as in Figures 3.5 and 3.6 except that the wind is assumed to be blowing at 100 m/sec toward the south and 100 m/sec toward the west. Figures 3.7 and 3.8 therefore correspond to Figures 3.1 and 3.2 except for the P-region velocity. Comparing the last four figures, we note that including neutral wind affects the number density profiles very little. The momentum transfer vector of the northbound electrojet, as expected, increases in magnitude and tilts toward the direction from which the wind blows.

It is apparent upon comparing Figures 3.5 – 3.8 with Figures 3.1 and 3.2 that the forward region momentum transfer is always directed antiparallel to the motion of the northbound successive dumping P-region.

Comparing Figure 3.6 with Figure 3.2 shows that the type (i) P-region loses none of its implicit AIW production capability as it moves southward such that equation (3.28) remains valid. However, the situation may be entirely different if the same P-region were to move through an ionosphere in which the local electric fields or winds were of a magnitude that caused equation (3.28) to be invalid.

Solutions of the second kind can be exhibited for a southbound type (i) P-region by assuming a lower value for the ambient southward electric field. This causes the impetus for ions to drift southward to be less. Figures 3.9 and 3.10 correspond to equations (3.26) through (3.27) and (3.31) through (3.32), respectively, and show the number density profiles and momentum transfer that would be expected if a P-region were successive dumping (Figure 3.9) or E x B driven (Figure 3.10) through an ionosphere in which the perpendicular electric field was 0.03 v/m and the wind was zero.

We note first the gross similarity of the profiles depicted in Figures 3.9 and 3.10. The wake of the northbound P-region is longer than the wake of the southbound P-region. The direction of momentum transfer is roughly antiparallel to the direction of electrojet motion in the northbound case but, in the southbound case, they are approximately parallel. The forward edge number density gradients of the southbound electrojet are generally higher than the corresponding gradients of the northbound electrojet.
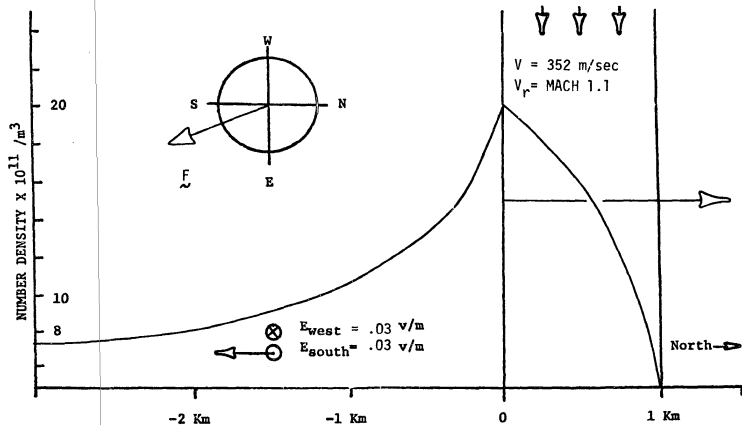
Fig. (3.5). Same as Fig. (3.1) except that the speed of the precipitation region is 352 m/sec and the wind velocity is zero. $\underset{\sim}{F}$ = (2.2E-5, S22°E).
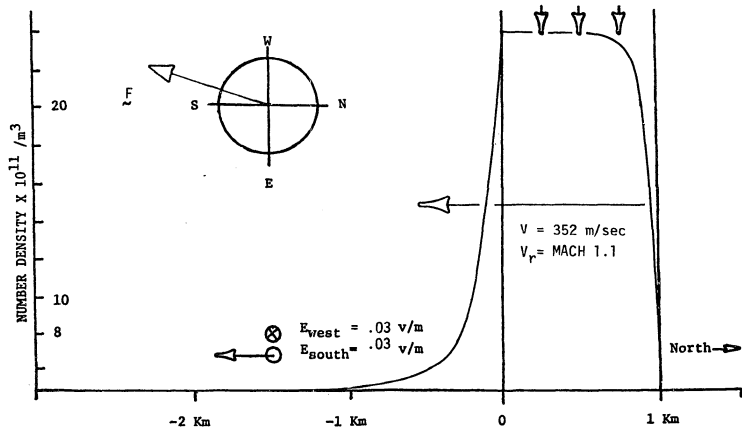
Fig. (3.6). Same as Fig. (3.2) except that the speed of the precipitation region is 352 m/sec and the wind velocity is zero. $\underset{\sim}{F} = (\gg 1.1E\text{-}3, \sim S19°W)$.
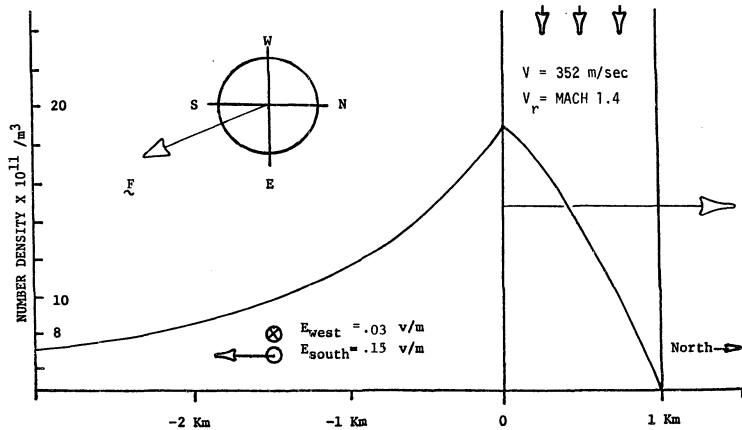
Fig. (3.7). Same as Fig. (3.1) except that the precipitation region speed is 352 m/sec. $\underset{\sim}{F}$ = (2.1E-3, S24°E).

105
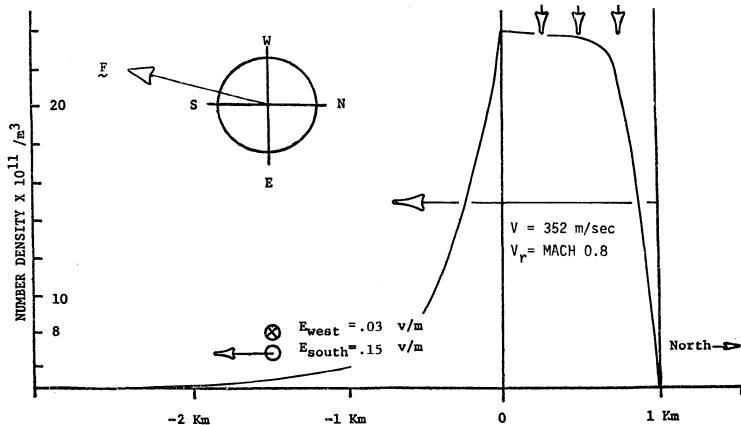
Fig. (3.8). Same as Fig. (3.2) except that the precipitation region speed is 352 m/sec. $\underset{\sim}{F} = (\gg 2.2E-3, \quad S15°W)$.

106
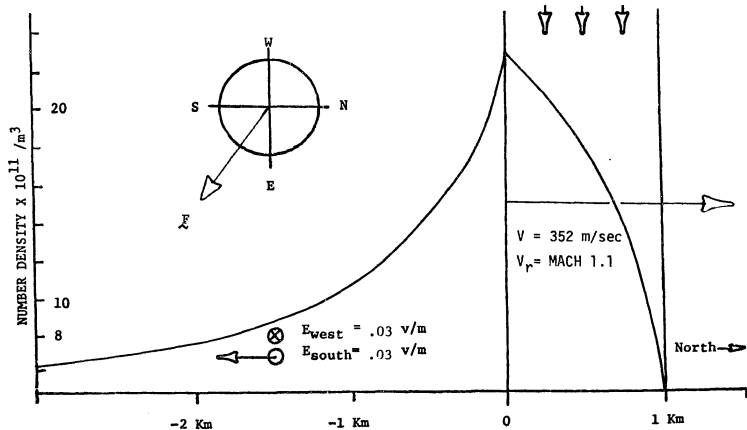
Fig. (3.9). Northbound precipitation region moving through an ionosphere with a low meridional component of the electric field and no wind. This profile corresponds to the case where southward motion is represented by solutions of the second kind. $\underset{\sim}{F} = (7.7E-4, S54°E)$.

107
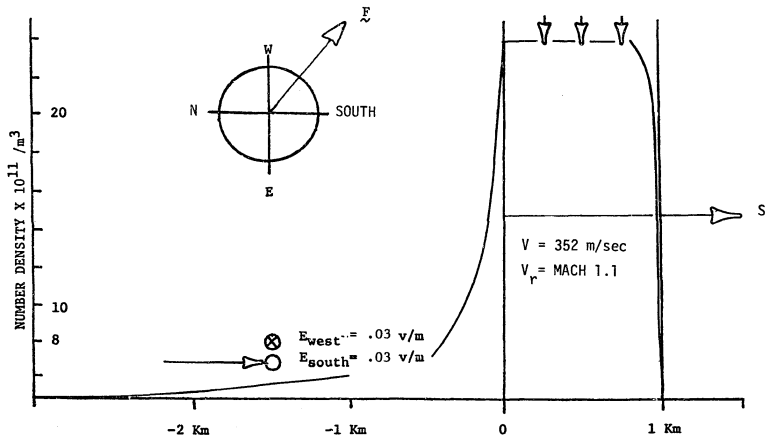
Fig. (3.10). Southbound precipitation region moving through an ionosphere with a low merid-
ional component of the electric field and no wind. Solutions of the second kind are indicated.
Note that in this figure, south is toward the right of the page. $\underset{\sim}{F}$ = (1.6E-3, S52°W).

For the same reasons as previously cited, the northbound successive dumping P-region should not produce an AIW which can later be associated with the direction of motion of the electrojet.

The southbound E x B driven P-region can, in principle, produce AIW which subsequently can be associated with the motion of the electrojet. However, the forward edge number density gradients of the solutions of the second kind can be expected to be much lower than the corresponding gradients of the solutions of the first kind. This again can be understood on the basis of how the first kind solutions were chosen.

When the plasma drift velocity within the interior region of the E x B driven electrojet is negative, solutions of the second kind are appropriate; when the drift is positive, solutions of the first kind are appropriate. Assuming a more realistic production function than the step function assumed for Figure 3.9 and 3.10, negative drift velocities would tend to decrease the forward edge number density gradients. Positive drifts would increase these gradients. Including pressure would only exacerbate this effect. Thus, if a P-region were E x B driven, such that equation (3.28) were valid, and it was associated with the production of an observable AIW, then the same E x B driven P-region would not be expected to be associated with an AIW, if it were moving such that equation (3.28) were invalid.

In view of this, it would appear that the validity of equation (3.28) and supersonic motion are representative of the sufficient conditions for the establishment of an asymmetrical mechanism for the production of auroral infrasound. It is emphasized that not all supersonic arcs which cross a station zenith are subsequently associated with

the reception of an AIW. Hence, a condition additional to supersonic motion, such as the validity of equation (3.28) is expected to pertain to the production of AIW by moving current distributions. The sufficient conditions for the production of an AIW will be dealt with in the next section.

The number density profiles and momentum transfer vectors depicted in Figures 3.1 - 3.10 are valid only insofar as previous mathematical assumptions have not been violated. Of particular concern is the assumption that $|(\gamma\ kT/mN)\ \partial N/\ \partial y\ | \ll\ |(e/m)E_y|$. In calculating the profiles, the term $(\ \gamma\ kT/mN)\ \partial N/\ \partial y$ was also calculated and compared to $(e/m)E_y$ for each case represented in the figures. In Figures 3.1 - 3.8, the maximum correspondence between the two terms was $(\gamma kT/mN)\ \partial N/\partial y = 6.4 \times 10^3$: $(e/m)E_y = 4.5 \times 10^5$. The criterion by which $(\gamma kT/mN)\ \partial N/\partial y$ was ignored is therefore valid for these cases. For the conditions implicit within Figures 3.9 and 3.10, the maximum correspondence was $(\gamma kT/mN)\ \partial N/\partial y = 1.3 \times 10^3$: $(e/m)E_y = 9.6 \times 10^4$, which occurred at the forward boundary of the southmoving electrojet (Figure 3.10). The term $(\gamma kT/mN)\ \partial N/\partial y$ might have been included in the development of the relevant equations. However, as Holt (1973) argues, inclusion of this term would tend to smooth the profile at the point where the term becomes important. Consequently, errors implicit in the overall profile should be negligible.

3.10 A DISCUSSION CONCERNING THE SUFFICIENT CONDITIONS FOR THE

     PRODUCTION OF AN AIW

    Wilson (1967) observationally established that a necessary condition for the production of an AIW was the supersonic motion of an auroral form. Later, Wilson (1969a) extended this observation to include the filamentary electrojet by using a simple line current induction model. Goodwin (1974) affirmed Wilson's (1969a) results by using an induction model which included the earth's conductivity. Swift (1973) theoretically derived the result that the supersonic motion of an arbitrary current distribution is necessary for the production of an AIW.

    Wilson (1971, 1972) observationally established that a further necessary condition for the production of an AIW was, apparently, that the supersonic, filamentary auroral form must move equatorward: Northward moving forms, however fast they traveled, did not seem to produce AIW.

    Within the framework of the theory developed here, it was found that filamentary electrojets moving poleward during negative bay conditions cannot produce associable AIW because the momentum transfer is both low and in a direction essentially antiparallel to the motion of the auroral form.

    The validity of equation (3.28) was found to be necessary for the production of AIW if the auroral precipitation region was E x B driven equatorward. The continuity equation solution showed that the leading boundary of an E x B driven flux tube, moving such that equation (3.28)

is valid, is characterized by much higher number density gradients than would be the case if the flux tube moved south such that equation (3.28) were not valid. In the context of Swift's (1973) AIW source equations, if the former auroral event could be said to produce an observable AIW, the latter could not.

Thus, to the extent that the movement of a filamentary electrojet can be described as steady state motion, the validity of equation (3.28) is necessary for the production of AIW. Also necessary for the production of an AIW is the supersonic motion of the electrojet. Together, these two necessary conditions are here proposed to represent sufficient conditions for the production of AIW by filamentary electrojets. Note that equation (3.28) applies to type (i) auroral precipitation events moving equatorward along the magnetic meridian.

For the special case of an electrojet that can be magnetically observed as filamentary as it moves over a station zenith, the theoretical and actual sufficient conditions should closely correspond. The theory was developed by using the unique geometrical and quasistationary properties of the filamentary electrojet.

However, electrojets which are not filamentary and which would not normally be described as in a steady state are often observed to produce AIW.

For a subclass of electrojets contained within this latter category the theoretical sufficient conditions herein proposed should still be applicable.

For instance, steady state, in the sense of the theory, is the condition where the produced ions have had sufficient time to travel

from one side of the P-region to the other. If the P-region changes in spacial character within a time span that allows ions to drift from one side to the other, the validity of equation (3.28) should still represent a necessary condition for the production of an AIW. (To estimate the time span, consider that Kim and Volkman (1963) measured the thickness of homogeneous arcs and found the mean to be 9.1 km. This would roughly correspond to the P-regions depicted in Figure 3.3, if the arcs were observed to move at the transverse speed of 1000 m/sec. Ion drift within the interior region of the primed frame for that case was found to be about 200 m/sec. Ions would, therefore, take approximately 45 sec to drift across the 9.1-km wide P-region. The fact that a given auroral form is not filamentary need not be of concern provided that the validity of equation (3.28) is examined at a symmetry point along the electrojet (i.e. $\partial/\partial x = 0$)).

Equation (3.28) may be written in a somewhat more general form. Consider that in the mathematical development the relations $E_{INy} = E_{oy}$ and $E_{INx} < 0.1 E_{INy}$ were used. The Hall current condition may be written as $E_{INx} = h E_{INy}$; $h < 0.1$. The parameter h can be thought of as a Hall current parameter. Inserting these into equation (3.28), along with the assumption that the rest frame neutral wind is zero it is found that

$$(3.33a) \qquad V < \frac{f - B_z h}{g} E_{oy}$$

where

$$f = m\nu/e + e/m\nu$$

(3.33b)

$$g = (m\nu/e)^2 + B_y^2 + B_z^2$$

Equation (3.33a) expresses the necessary condition for the production of AIW as a function which relates the observed velocity of the auroral form southward to the electric field component in the direction of motion and perpendicular to the form. It is implicit that the auroral form arises in consequence of an E x B driven P-region.

To summarize, in this section sufficient conditions for the production of AIW have been proposed. These are:

1) The AIW source must be a type (i) P-region;

2) The AIW source must move supersonically;

3) The AIW source speed and the magnitude of the applied electric field in the direction of motion must be such that equation (3.28) is valid.

We see that the proposed sufficient conditions preclude the production of AIW by all successive dumping events, including those dumping southward, if any in fact exist.

3.11 SUMMARY AND CONCLUDING COMMENTS

A model depicting the dynamics of the ionization associated with moving auroral arcs has been developed. Principle to the development was the argument that northward motion occurs because northbound pre-

cipitation is dumped along successive magnetic field lines. As a result, there is no objective component of plasma velocity in the northward direction. Southward motion was said to be related to precipitation flux tubes E x B driven in that direction by the known or inferred ionospheric and magnetospheric electric fields.

Utilizing the E x B driven flux tube as a model for southward motion and successive dumping as a model for northward motion, the momentum transfer and continuity equations were simplified and solved.

From the solutions of these fundamental equations, it was argued that if the so-called solution of the first kind, which pertain to southward motion, were held in correspondence with the production of an AIW, the solutions of the second kind, which pertain to some southward motion and all northward motion, could not be. This argument was based, in part, on the observation that only certain supersonic arcs are subsequently associated with the reception of an AIW.

Model sufficient conditions for the production of an AIW were proposed. On the basis of an argument which stipulated that the auroral precipitation regions were relatively narrow and in motion long enough to move across the P-region, it was proposed that the model sufficient conditions appropriately represented the actual conditions mandatory for the production of an AIW.

The theory and the corresponding model developed should be able to be checked by experiment. For instance, the model predicts that strong arcs that rapidly move poleward during the negative bay conditions of

a magnetic substorm are characterized by rather long ionization wakes. In contrast, the ionization associated with the southbound E x B driven arc is relatively more confined to the precipitation region. Hence, radar, if it cannot see the northbound arc's wake directly, should be able to statistically determine that north-moving arcs are ionization- ally thicker than the corresponding south-moving arcs.

Radar can also be used to check the validity of the proposed suf- ficient conditions for the production of an AIW. Turning the radar toward the east or west, line-of-sight ion drifts can be determined. Assuming the validity of the $\underset{\sim}{E} = (\underset{\sim}{v_i} \times \underset{\sim}{B})/B^2$ relation, the meridional component of the electric field may be obtained. This meridional com- ponent is the ambient or applied field perpendicular to southward moving arcs. Supportive all-sky camera analyses can be used to obtain the arc speed V where, according to Kelly et al. (1971), the majority of south- bound arcs that occur during negative bay conditions are E x B driven and, hence, are type (i) events.

The component of the electric field perpendicular to the arc and the known arc velocity can be inserted into the proposed sufficient condition that relates these two parameters (equation (3.33a)). If it is found that the proposed sufficient conditions are statistically valid prior to the reception of an AIW and invalid during those times when no AIW are received, the theory and the model developed here would be substantially corroborated.

CHAPTER IV

AN OVERALL SUMMARY OF THE RESULTS OBTAINED

4.1 SUMMARY

One thrust of this work is to examine the asymmetry observed in the
reception of AIW, a problem stated in Chapter I. A review of research
germane to the problem is therein given. It is found that the AIW
reception asymmetry is explainable in terms of either anisotropic
acoustic propagation or some property intrinsic to the AIW generation
mechanism.

In Chapter II, it is assumed at the outset that the AIW reception
asymmetry is a consequence of an acoustic anisotropy of the polar at-
mosphere. Since infrasound spectrally similar to AIW have been observed
to propagate poleward in the lower two polar sound channels, during
magnetically and/or AIW active or inactive periods, the atmosphere below
the mesopause is eliminated as the possible seat of the assumed ani-
sotropy. On that basis, it is concluded that the anisotropy, if it is
to exist at all, must exist in the E-region where AIW originate.

Mean wind pattern profiles above College, Alaska, are presented.
The profiles below 80 km are constructed from data given in the
Handbook of Geophysics (1960) and CIRA (1965). Above the 80-km level it
is found that the wind is highly variable both in direction and magni-
tude. However, observations by Hook (1970) and Rees (1971) indicated
that within 2-3 hours of the onset of a magnetic substorm, significant

117

winds blowing in the general direction of the auroral electrojet can be
assumed. Thus, an antisunward wind in the night-side hemisphere can be
assumed to persistently blow during many AIW active periods.

The behavior of acoustic wave normals in the presence of wind is
next examined. It is shown that a wind layer can represent an acoustic
obstacle. It is also shown that wind can reflect or refract AIW. As a
result, wind can account for, on some occasions, the observation that
many supersonic auroral forms are not associated with the subsequent
reception of AIW. However, on the basis of the variability of the wind
and on the basis of the wave normal analysis, it is clear that the wind
cannot account for the AIW reception asymmetry in general.

With wind eliminated as the general source of the AIW reception
asymmetry, it follows that AIW must be produced preferentially with
respect to the north-south direction. Swift (1973) has shown that the
production of infrasound by moving current distributions is a function
of the ionization number density gradients. The differences expected in
these gradients, and in the momentum transfer, associated with a north-
as opposed to south-moving electrojet is examined in Chapter III.

Direct observations concerning the AIW reception asymmetry were
conducted at Inuvik, N.W.T., Canada by Wilson (1971, 1972). These
observations implicate the so-called filamentary electrojet (Wilson,
1969a; Goodwin, 1974) as being representative of the apparent asymmetry
in the production of auroral infrasound.

The relationship between the filamentary electrojet, the visible
arc and the parent precipitation region (P-region), is examined. It is

found that the electrojet and arc are manifestations of the P-region; the location and motion of one essentially duplicating the location and motion of the other two.

The motion of P-regions north as opposed to south is discussed. On the basis of the observations of Kelly et al., (1971), and on the basis of magnetospheric convection theory (see for instance, Mozer and Manka, 1971), it is argued that rapid poleward expansions that occur during the negative bays of magnetic substorms are successive dumping precipitation events: Equatorward expansions, it is argued, are predominantly the results of E x B driven precipitation flux tubes. Precipitation which successively dumps poleward is labeled the type (ii) event and corresponds to Bostrom's (1964) "case 1" current system. The E x B driven flux tube is labeled as a type (i) event and corresponds to Bostrom's (1964) "case 2" current system.

The filamentary electrojet is shown to be an easily visualized phenomenon which can occur in conjunction with either a type (i) or (ii) P-region.

The electrojet and E-region are considered as composed of a three-fluid plasma. The plasma is taken to be singly ionized and quasi-neutral. The equation of motion of the charged component of the plasma (Alfvén and Falthämmar, 1963) is simplified to result in the ionic momentum transfer equation (cf. Appendix II).

The observed length and temporal stability of the filamentary electrojet and certain symmetry conditions are used to simplify the ionic momentum transfer equation. Further simplifications are made by

comparing the order of magnitude of each term of the component momentum transfer equation with each other term.

Using the type (i) and (ii) events as models for the E x B driven and successive dumping P-regions, the continuity equation is solved. The momentum transfer equation solution for ion velocity provides the functional form for the coefficients of ion number density in the continuity equation. Analytic solutions for the continuity equation of two kinds are thus arrived at. First kind solutions correspond to the case where E x B driven electrojets are moving equatorward such that a large component of electric field is perpendicular to the electrojet axis. Second kind solutions correspond to electrojets arising from successive dumping P-regions and also to electrojets which are E x B driven but with a relatively small component of electric field perpendicular to the electrojet axis.

Parameter values are adopted and ion number density profiles are calculated. In the discussion accompanying these profiles it is shown that when solutions of the first kind pertain, ion number density gradients increase as the electrojet moves. It is argued that this will occur irrespective of the functional form of the precipitation flux profile. It is shown that when second kind solutions pertain, ion number density gradients decrease as the electrojet moves faster. It is argued that this dynamical behavior is also independent of the precipitation flux profile.

This dynamical behavior of the charged component of the P-region plasma is shown to be a consequence of the difference between the ionic impetus to drift in the direction of the applied electric field and the

impetus for ions to drift in the E x B direction. Inside the electrojet, drift in these two directions can be contrary. First kind solutions pertain when the net P-region ion drift is in the direction of electrojet motion. Second kind solutions pertain when the net P-region ion drift is antiparallel to the electrojet motion.

Swift (1973) has shown that the magnitude of the acoustic pressure perturbation produced by a moving electrojet source depends primarily on the leading edge ionization number density gradients. Electrojets which move according to first kind solutions are characterized by number density gradients along the leading edge which are orders of magnitude greater than the leading edge gradients of electrojets which move such that solutions of the second kind pertain. Thus, it is argued that if "first kind electrojets" are said to produce observable AIW, then "second kind electrojets" produce much less than observable AIW.

Moreover, it is shown that northbound successive dumping P-regions and the associated electrojets transfer momentum in a direction generally antiparallel to the motion of the P-region. From this it is concluded that if the northbound successive dumping event produces an AIW, the AIW cannot be associated with the electrojet or arc in the usual sense. It is further shown that southbound E x B driven auroral forms transfer momentum in the direction of motion and, as a result, if they produced AIW, the motion of these AIW can be associated with the motion of the electrojet or arc.

Sufficient conditions for the production of AIW are proposed.

4.2 A DISCUSSION CONCERNING THE ASSUMPTIONS USED AND CONCLUDING

COMMENTS

Plane waves are used to assess the magnitude of the acoustic

anisotropy represented by wind. It is argued that, although plane waves

are not representative of AIW, if a plane wave were not expected to

propagate in a given direction through wind, neither would AIW be ex-

pected to propagate in that direction. It is moreover, argued that the

behavior of plane wave normals in the presence of wind duplicate, in

the first order sense, the behavior of the corresponding AIW wave

normals.

It is thought that the argument concerning the correspondence

between AIW and plane waves is the weakest point of Chapter II. How-

ever, the contradiction of this argument is not tenable at all. There-

fore, the conclusions reached in Chapter II are logically consistent

and, as a result, should be sufficiently representative to justify

application to the first order behavior of AIW as they propagate through

the actual wind and temperature stratified atmosphere.

In Chapter III, the equation of motion for the charged component of

plasma is shown to be reducible to the ionic momentum transfer equation.

The simplifications depend on order of magnitude differences in the col-

lision frequencies at auroral altitudes (Nicolet, 1953; Dalgarno, 1961;

Bostrom, 1964) and on the mass differential between ions and electrons.

Steady-state conditions are also assumed.

The ionic momentum transfer and continuity equation are solved by
assuming a model which depicts arcs moving north as arising from suc-
cessive dumping precipitation whereas arcs moving south arise from
precipitation flux tubes, E x B driven in that direction. Steady-state
conditions are assumed. It is also assumed that the precipitation flux
profile can be represented as a step function.

Each assumption used in Chapter III was discussed in context. Given
these discussions, it is thought that the successive dumping-E x B
driven assumption is the weakest. This assumption depends on the
validity of magnetospheric convection theory. In as much as there is no
substantial reason to doubt magnetospheric convection, the successive
dumping – E x B driven assumption should substantively represent the
actual motion of arcs north as opposed to south. Accordingly, the
results of Chapter III should prove to be largely correct in substance
if not in detail.

Therefore, as the title implies, the primary contribution associ-
ated with this thesis is the presentation of an argument which estab-
lishes the mechanism whereby auroral arcs moving north as opposed to
south may be characterized by different ionization profiles, thus demon-
strating the existence of a motion-related asymmetry. If the theory
presented herein holds up under the scrutiny of experiment, the theory
should be of some value in furthering our understanding of the auroral
phenomenon, as well as of value in answering some questions, not the
least of which is the question of the observed asymmetry in the re-
ception of AIW.

APPENDIX I

FOURIER SPECTRUM OF TYPICAL AIW

A Geotech-teledyne TC-200 digital data acquisition system has been in operation at College, Alaska at various times during the years 1969-1974. The significant feature of the TC-200 system is the bandpass. It has a flat response to atmospheric waves with periods between 1 sec and 1000 sec. Consequently, the system produces very little ringing when monitoring an incoming AIW. Further information concerning the TC-200 can be obtained from Herrin and McDonald (1971). The College microphone array is described by Nichparenko (1967).

A spectrum analysis of certain typical AIW observed by the COL TC-200 during 1970 has been performed.

Figures (A-I.1) and (A-I.2) show examples of the spectrum analysis performed on the AIW wavepackets that were received at COL, at the time indicated. The uppermost plot depicted in each figure is the analog version of an AIW being monitored on four separate microphones and filtered by the N7 bandpass (Nichparenko, 1967). The four plots have been time shifted with respect to each other so as to conform to a "best fit" coherence scheme. Using the time shift and the microphone coordinates, an AIW trace velocity and the arrival angle is obtained. The trace velocity and arrival angle are indicated beside the corresponding analog plot of each figure. The appropriate time shift of each event was inserted into the digital processing programs of Herrin and McDonald (1971). The computer read the digital version of the analog

124
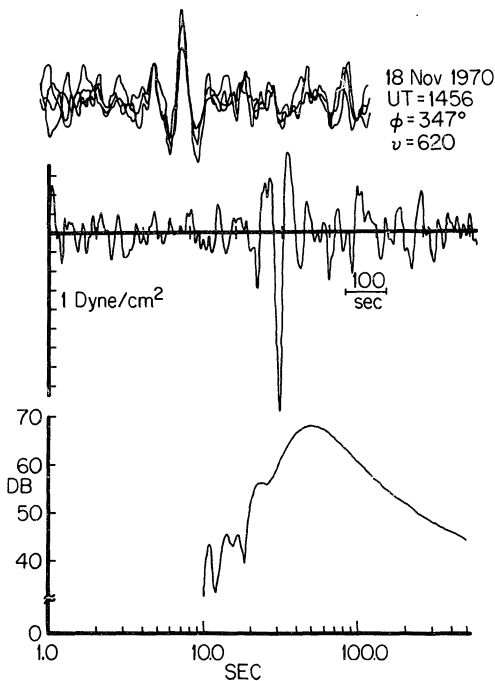
Fig. (A-I.1). Uppermost plot corresponds to an AIW monitored on four microphones, filtered on the N7 bandpass and time shifted for coherence. The center plot is of the same AIW monitored on the TC-200 bandpass then mathematically filtered using the coherence parameters obtained from the uppermost plot. The lower plot is of db above the mean for each Fourier component of the center figure. The parameters ϕ and v are the arrival azimuth and trace speed of the AIW.

28 Dec 1970
UT=1908
ϕ=345°
υ=505

100
sec
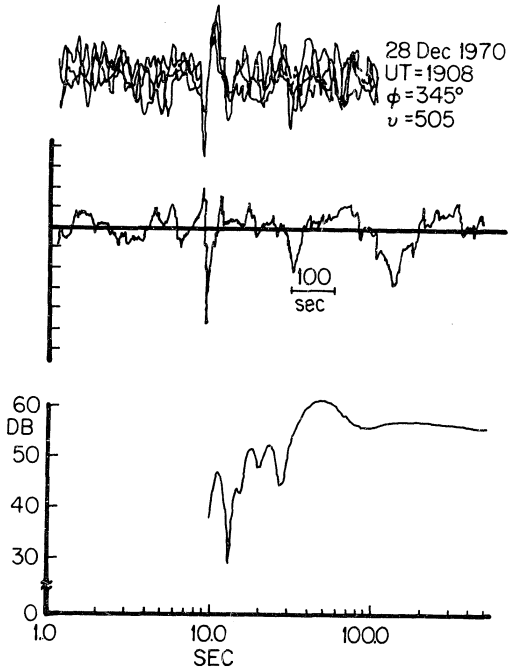
Fig. (A-I.2). Same as Fig. (A-I.1) expect different AIW.

plot using the specified time shift between each of the four channels of microphone data, segmented it, transformed it to the frequency domain and then averaged it (Welch, 1967). An average analog plot thus obtained is shown for each AIW event at the center of Figures (A-I.1) and (A-I.2). The amplitude of the Fourier components needed to construct the waveform contained within the data window were compared with the average window amplitude. A plot of decibels above mean was constructed for each Fourier component amplitude. This version of the data is shown by the lowermost plot of each figure.

From Figures (A-I.1) and (A-I.2), it is seen that the dominant Fourier components of the typical AIW lie within the period range between 40 and 80 sec. This result is in agreement with the conclusions reached by Maeda and Young (1966). Being entirely within the acoustic mode, waves with this range of periods would imply wavelengths of approximately 12 km to 24 km.

THE EQUATION OF MOTION OF THE CHARGED COMPONENT

OF A THREE-FLUID PLASMA SIMPLIFIED FOR APPLICATION TO AURORA

The equation of motion for the charged component of a three-fluid model plasma is given by Alfvén and Falthämmar (1963, see page 176) as:

$$(A-II.1) \qquad \rho c \, \frac{dv_c}{dt} \;=\; \underset{\sim}{i} \times \underset{\sim}{B} \;-\; \nabla(P_e + P_i) + \rho_c \, \underset{\sim}{g}$$

$$- \, \rho_c \, \nu_{in} \, [(1 + \frac{m_e}{m_i} \, \frac{\nu_{en}}{\nu_{in}}) \, (\underset{\sim}{V}_c - \underset{\sim}{V}_n)$$

$$- \frac{m_c}{m_i} \, (\frac{\nu_{en}}{\nu_{in}} - 1) \, \underset{\sim}{i} \, / \, |e| \, N]$$

where
$$\rho_c \;=\; N(m_i + m_e)$$

$$\rho_c \underset{\sim}{V}_c = N(m_i \underset{\sim}{V}_i + m_e \underset{\sim}{V}_e)$$

The notation used in equation (A-II.1) is defined in the present text (cf. section 3.1).

It is known that $(m_e/m_i) \, \theta \, 10^{-5}$ (θ is read "on the order of"). According to equations (3.5e) and the parameter values as specified in the present text, $|\nu_{in}| \; \theta \; 10^3$, $|\nu_{en}| \theta \, 10^5$ and $\nu_{ei} = 10\text{-}10^2/\text{sec}$ (cf. section 3.4). Consequently, $(\nu_{en}/\nu_{in}) \theta \, 10^2$, $\rho_c \simeq N m_i = \rho_i$ and $\rho_c \underset{\sim}{V}_i \simeq N m_i \underset{\sim}{V}_i = \rho_i \underset{\sim}{V}_i$. Equation (A-II.1) may therefore be approximated by,

128

$$(A-II.2) \quad \rho i \frac{d\underset{\sim}{v_i}}{dt} \simeq (\underset{\sim}{j} \times \underset{\sim}{B} + \frac{\nu_{en}}{|e|} \frac{m_e}{} \underset{\sim}{j}) - \nabla(P_e + P_i)$$

$$- \rho_i \nu_{in} (\underset{\sim}{v_i} + \underset{\sim}{v_n}) + \rho_i \underset{\sim}{g}$$

The generalized Ohm's law for the model plasma under consideration may be written as

$$(A-II.3) \quad \underset{\sim}{E}_{eff} = n[\underset{\sim}{j} + \frac{\omega e}{\nu e} (\underset{\sim}{j} \times \underset{\sim}{B}/B) + \frac{1}{\nu_e} \frac{\partial}{\partial t} \underset{\sim}{j}]$$

with

$$(A-II.4) \quad \underset{\sim}{E}_{eff} = \underset{\sim}{E} + (\underset{\sim}{v_c} \times \underset{\sim}{B}) + \frac{1}{|e|N} (\nabla P_e - \frac{m_e}{m_i} \nabla P_i) + \beta(\underset{\sim}{v_c} - \underset{\sim}{v_n})$$

where

(a) $\eta = m_e \nu_e / e^2 N$

(b) $\nu_e = \nu_{ei} + \nu_{en} + \nu_{in} (m_e/m_i)$

(c) $\beta = (m_e \vec{/}|e|) (\nu_{en} - \nu_{in})$

(Alfvén and Falthämmar, 1963, see page 178).

With the given order of magnitudes for m_e/m_i and the various $|\nu|$,

$$\nu_e = \nu_{en} (\frac{\nu_{ei}}{\nu_{en}} + 1 + \frac{m_e}{m_i} \frac{\nu_{in}}{\nu_{en}})$$

$$\simeq \nu_{en}$$

in which case, Equation (A-II.3) may be written

$$(\text{A-II.6}) \qquad |e| \, N \, \underset{\sim}{E}_{\text{eff}} \; = \; \underset{\sim}{i} \times \underset{\sim}{B} + \frac{\nu_{en} \, m_e}{|e|} \; \underset{\sim}{i}$$

where a steady-state current density has been assumed.

Inserting Equation (A-II.6) into equation (A-II.2) shows that

$$\rho_i \, \frac{d\underset{\sim}{v_i}}{dt} \approx |e| \, N \, \underset{\sim}{E}_{\text{eff}} \; - \; \nabla(P_e + P_i) - \rho_i \, \nu_{in} \; (\underset{\sim}{v_i} + \underset{\sim}{v_n}) + \rho_i \, \underset{\sim}{g}$$

Or, using equations (A-II.4) and (A-II.5c),

$$\rho_i \, \frac{d\underset{\sim}{v_i}}{dt} \; = \; |e| \, N \, \underset{\sim}{E} \; + \; |e| \, N \, (\underset{\sim}{v_c} \times \underset{\sim}{B}) + \nabla P_e - \frac{m_e}{m_i} \, \nabla P_i$$

$$+ \, m_e \, N \, (\nu_{en} - \nu_{in}) \; (\underset{\sim}{v_c} - \underset{\sim}{v_n}) - \nabla P_e - \nabla P_i$$

$$- \, \rho_i \, \nu_{in} \; (\underset{\sim}{v_i} - \underset{\sim}{v_n}) + \rho_i \, \underset{\sim}{g}$$

However, $\rho_c = \rho_i + \rho_e \simeq N m_i$ and $\rho_c v_c \simeq \rho_i v_i$. Hence,

$$\rho_i \, \frac{d\underset{\sim}{v_i}}{dt} \approx \rho_i \frac{|e|}{m_i} \, \underset{\sim}{E} \; + \; \rho_i \, \frac{|e|}{m_i} \; (\underset{\sim}{v_i} \times \underset{\sim}{B}) - (1 + \frac{m_e}{m_i}) \, \nabla P_i$$

$$+ \, (\rho_e \, \nu_{en} - \rho_e \, \nu_{in} - \rho_i \nu_{in})(\underset{\sim}{v_i} - \underset{\sim}{v_n}) \; + \rho_i \, \underset{\sim}{g}$$

But, $(1 + m_e/m_i) \simeq 1$ and

$$(\rho_e \, \nu_{en} - \rho_e \, \nu_{in} - \rho_i \, \nu_{in}) = \rho_i \, \nu_{in} \left(\frac{\rho_e}{\rho_i} \frac{\nu_{en}}{\nu_{in}} - \frac{\rho_e}{\rho_i} - 1 \right)$$

$$\simeq \rho_i \, \nu_{in}$$

Therefore,

(A-II.7) $$\rho_i \frac{d\underset{\sim}{v}_i}{dt} \simeq_i \frac{|e|}{m_i} \, \underset{\sim}{E} + \rho_i \frac{|e|}{m_i} \, (\underset{\sim}{v}_i \times \underset{\sim}{B}) - \nabla P_i$$

$$- \rho_i \, \nu_{in} \, (\underset{\sim}{v}_i - \underset{\sim}{v}_n) + \rho_i \, \underset{\sim}{g}$$

To simplify further $\rho_i \underset{\sim}{g} = - \rho_i g \hat{e}_z$, where $\hat{e}_z$ is the unit vector in the vertical direction, can be compared to $\rho_i (|e| / m_i) \, v_{ix} B_y \, \hat{e}_z$, where v_{ix} is the ion speed along $\underset{\sim}{i}$. We may, then, write,

$$[- \rho_i g + \rho_i \, (|e|/m_i) \, v_{ix} \, B_y \,] \, \hat{e}_z$$

as $$\rho_i \, (|e|/m_i) \, B_y \, v_{ix} \, \left(1 - \frac{gm_i}{|e| \, B_y \, v_{ix}} \right) \, \hat{e}_z$$

But

$$\left(1 - \frac{gm_i}{|e| \, B_y \, v_{ix}} \right) \simeq \left(\frac{1 - 8 \times 10^{-2}}{v_{ix}} \right)$$

Thus, for any reasonable non-zero value of v_{ix}, equation (A-II.7) may be written as

$$(\text{A-II.8}) \quad \rho_i \, \frac{d\underset{\sim}{V}_i}{dt} \approx \rho_i \, \frac{|e|}{m_i} \, \underset{\sim}{E} \, + \rho_i \, \frac{|E|}{m_i} \, (\underset{\sim}{V}_i \times \underset{\sim}{B}) - \nabla P_i - \rho_i \nu_{in} (\underset{\sim}{V}_i - \underset{\sim}{V}_n)$$

which is the ionic momentum transfer equation for a three-fluid model plasma in which there is a steady current. The plasma is considered quasi-neutral and composed of singly ionized species.

BIBLIOGRAPHY

Akasofu, S.-I., S. Chapman, and C.-I. Meng, The polar electrojet,
    J. Atmos. Terrest. Phys., 27, 1275, 1965.

Alfvén, H., and C.-G. Falthämmer, Cosmical Electrodynamics, Oxford
    University Press, Great Britain, 1963.

Blokhintzev, D., The propagation of sound in an inhomogeneous moving
    medium II. J. Acoust. Soc., Am., 18, 329, 1945.

Bostrom, R., A model of the auroral electrojets, J. Geophys. Res.,
    69, 4983, 1964.

Bryant, D. A., G. M. Courtier, G. Skovli, H. R. Lindalen, K. Aarsnes,
    and K. Maseide, Electron density and electron flux in a glow
    aurora, J. Atmos. Terrest. Phys., 32, 1695, 1970.

Chimonas, G., Infrasonic waves generated by auroral currents, Planet.
    Space Sci., 18, 591, 1970.

Chimonas, G. and W. R. Peltier, The bow wave generated by an auroral
    arc in supersonic motion, Planet. Space Sci., 18, 599, 1970.

Chrzanowski, P., G. Greene, K. T. Lemmon, and J. M. Young, Traveling
    pressure waves associated with geomagnetic activity, J. Geo-
    phys. Res., 66, 3727, 1961.

CIRA 1965, COSPAR International reference atmosphere, M. Holland
    Pub. Co., Amsterdam, 1965.

Clemmow, P. C., M. A. Johnson, and K. Weekes, Rept. Phys. Soc. Conf.
    Phys. Ionosphere, 136-139, London, 1955.

Dalgarno, A., Charged particles in the upper atmosphere, Ann. Geophys.,
    17, 16, 1961.

Diamond, M., Sound channels in the atmosphere, J. Geophys. Res., 68,
    3459, 1963,

Donn, W. L., and W. Ewing, Atmospheric waves from nuclear explosions,
    J. Geophys. Res., 67, 1855, 1962.

133

Fedder, J. A., and P. M. Banks, University of California, California, U.S.A., unpublished, 1972.

Fel'dshtevn, Ya.I., Some problems concerning the morphology of auroras and magnetic disturbance at high latitudes, Geomag. and Aero., 3, 183, 1963.

Goerke, V. H., and M. W. Woodward, Infrasonic observation of a severe weather system, Mon., Weather Rev., 94, 395, 1966.

Goerke, V. H., J. M. Young, and R. K. Cook, Infrasonic observations of the May 16, 1963 volcanic explosion on the island of Bali, J. Geophys. Res., 70, 6017, 1965.

Goodwin, P. A., Auroral electrojet velocities from an induction model, M.S. Thesis, Geophysical Institute, University of Alaska, Fairbanks, Alaska, 99701, 1974.

Green, G. E., and J. Howard, Natural infrasound: a one-year global study, NOAA TR ERL 317-WPL 37, 1975.

Gregory, J. B., and A. H. Manson, Winds and wave motions to 110 km at mid-latitudes, II. Mean winds at 52 N, 1969-73, J. Atmos. Sci., 32, 1667, 1975.

Handbook of Geophysics, U. S. Air Force, MacMillan Co., New York, 5-1, 1960.

Harkrider, D. G., Theoretical and observed acoustic-gravity waves from explosive sources in the atmosphere, J. Geophys. Res., 69, 5295, 1965.

Herrin, E., and J. A. McDonald, A digital system for the acquisition and processing of geoacoustic data, Geophys. J. R. Astro. Soc., 26, 13, 1971.

Holt, O., University of Tromso, Auroral Observatory, unpublished, 1973.

Hook, J. L., Winds at the 75-110 km level at College, Alaska, Planet. Space Sci., 18, 1623, 1970.

Johnson, C. Y., E. B Meadows, and J. C. Holmes, Ion composition of the arctic ionosphere, J. Geophys. Res., 63, 443, 1958.

Johnson, F. S., Structure of the upper atmosphere, Satellite Environment Handbook, Ed. F. S. Johnson, Stanford University Press, Stanford, Ca., 9–24, 1961.

Kato, S., Theory of movement of irregularities in the upper atmosphere, Planet. Space Sci., 11, 823, 1963.

Kato, S., Theory of movement of irregularities in the ionosphere, Space Sci. Rev., 4, 223, 1964.

Kelly, M. C., J. A. Starr, and F. S. Mozer, Relationship between magnetospheric electric fields and the motion of auroral forms, J. Geophys. Res., 76, 5269, 1971.

Kim, J. S., and R. A. Volkman, Thickness of zenithal auroral arc over Fort Churchill, Canada, J. Geophys. Res., 68, 3187, 1963.

Kornhauser, E. T., Ray theory for moving fluids, J. Acoust. Soc. Am., 25, 945, 1953.

Landau, L. D., and E. M Lifschitz, Fluid Mechanics, Addison-Wesley, Reading, Mass., 256, 1959.

Love, A. E. H., Some Problems of Geodynamics, Cambridge University Press, London, 144, 1911.

Maeda, K., and T. Watanabe, Infrasonic waves from the auroral zone, NASA TN D-2138, 1964.

Maeda, K., and J. M. Young, Propagation of the pressure waves produced by auroras, J. Geomag. and Geoelec., 18, 275, 1966.

Mende, S. B., Experimental investigation of electric fields parallel to the magnetic field in the auroral ionosphere, J. Geophys. Res., 73, 991, 1968.

Morse, P. M., and K. U. Ingrad, Theoretical Acoustics, McGraw-Hill Book Co, N.Y. 698FF, 1968.

Mozer, F. S., and R. H. Manka, Magnetospheric electric field properties deduced from simultaneous balloon flights, J. Geophys. Res., 76, 1697, 1971.

Nichparenko, S., Aurorally associated infrasonic waves, M.S. Thesis, Geophysical Institute, University of Alaska, Fairbanks, Alaska, 99701, unpublished, 1967.

Nicolet, M., The collision frequency of electrons in the ionosphere, J. Atmos. Terrest. Phys., 3, 200, 1953.

Pfeffer, R. L., and J. Zarichny, Acoustic-gravity wave propagation
    in an atmosphere with two sound channels, Geofis. Pura e Appl.,
    55, 175, 1963.

Piddington, J. H., Geomagnetic storms, auroras and associated effects,
    Space Sci. Rev., 3, 724, 1964.

Pidmore-Brown, D. C., Sound propagation in a temperature- and wind-
    stratified medium, J. Acoust. Soc. Am., 34, 438, 1962.

Pierce, A. D., Propagation of acoustic-gravity waves in a temperature-
    and wind-stratified atmosphere, J. Acoust. Soc. Am., 37, 218, 1965.

Press, F., and D. Harkrider, Propagation of acoustic-gravity waves
    in the atmosphere, J. Geophys. Res., 67, 3889, 1962.

Rayliegh, J. W. S., Theory of Sound, II, Dover Publications, New York,
    133, 1945.

Ress, D., Ionospheric winds in the auroral zone, J. Brit. Interplant.
    Soc., 24, 233, 1971.

Swift, D. W., The generation of infrasonic waves by auroral electrojets,
    J. Geophys. Res., 78, 8205, 1973.

Tolstoy, I., Shallow water test of the theory of layered wave guides,
    J. Acoust. Soc. Am., 30, 348, 1957.

Weins, R., and G. Rostoker, The growth phase and sector structure
    of the polar magnetic substorm, Killam Earth Sciences, Univer-
    sity of Alberta, Edmonton, Alberta, Canada.

Welch, P. D., The use of fast fourier transforms for the estimation
    of power spectra: a method based on time averaging over short
    modified periodograms, Trans. IEEE, AU-15, 70, 1967.

Wescott, E. M., J. D. Stolarik, and J. P. Heppner, Electric fields in
    the vicinity of auroral forms from motions of barium vapor re-
    leases, J. Geophys. Res., 74, 3469, 1969.

Wilson, C. R., Infrasonic pressure waves from the aurora: a shock
    wave model, Nature, 216, 131, 1967.

Wilson, C. R., Infrasonic waves from moving auroral electrojets,
    Planet. Space Sci., 17, 1107, 1969a.

Wilson, C. R., Auroral infrasonic waves, J. Geophys. Res., 74, 1812, 1969b.

Wilson, C. R., Two station auroral infrasonic wave observations, Planet. Space Sci., 17, 1817, 1969c.

Wilson, C. R., Auroral infrasonic waves and poleward expansions of auroral substorms at Inuvik, N.W.T., Canada, Geophys. J. R. Astro. Soc., 26, 179, 1971.

Wilson, C. R., Auroral infrasonic wave-generation mechanism, J. Geophys. Res., 77, 1820, 1972.

Wilson, C. R., Trans-auroral zone auroral infrasonic wave observations, Planet. Space Sci., 22, 151, 1974.

Wilson, C. R., Infrasonic wave generation by aurora, J. Atmos. Terrest. Phys., 37, 973, 1975.

Wilson, C. R., and R. B. Forbes, Infrasonic waves from Alaskan volcanic eruptions, J. Geophys. Res., 74, 4511, 1969.

Wilson, C. R., and S. Nichparenko, Infrasonic waves and auroral activity, Nature, 214, 1299, 1967.